The influence of soil chemistry on branched tetraether lipids in mid- and high latitude soils: Implications for brGDGT- based paleothermometry

C. De Jonge [a,b,*], E.E. Kuramae [c,d], D. Radujković [a], J.T. Weedon [a,e], I.A. Janssens [a], F. Peterse [f]

[a] *University of Antwerp, Dept. of Biology, 2610 Wilrijk, Belgium*
[b] *ETH Zürich, Geological Institute, 8092 Zürich, Switzerland*
[c] *Netherlands Institute of Ecology (NIOO-KNAW), Dept. Microbial Ecology, 6700 AB Wageningen, the Netherlands*
[d] *Utrecht University, Dept. of Biology, 3584 CH Utrecht, the Netherlands*
[e] *Vrije Universiteit Amsterdam, Dept. of Ecological Science, 1081 HV Amsterdam, the Netherlands*
[f] *Utrecht University, Dept. of Earth Sciences, 3584 CB Utrecht, the Netherlands*

Abstract

Branched glycerol dialkyl glycerol tetraethers (BrGDGTs) are a suite of orphan bacterial membrane lipids commonly used as paleo-environmental proxies for mean annual air temperature (MAT) and pH. Recent calibrations between the Methylation of Branched Tetraethers index (MBT$'_{5ME}$) and MAT, based on modern surface soils (including peats), show a considerable amount of scatter, especially in mid- and high latitude soils, suggesting that brGDGT signals are influenced by additional environmental and/or biological controls at these sites. Here we test the impact of soil chemical gradients and bacterial community changes (16S rDNA sequence-based) on brGDGT distributions at two grasslands sites (Ossenkampen [NL], ForHot [IS]), and one agricultural site (Craibstone [UK]). In addition to the variation in soil chemistry, the ForHot site experiences belowground warming. Of the studied edaphic parameters, soil pH is the primary factor that explains simultaneous changes in both the bacterial community composition and the brGDGT distribution. Variations in the MBT$'_{5ME}$ at two sites without soil warming indeed correlate strongly to soil pH (r = 0.9–1.0, pH = 4.5–7.3), whereas pH explains part of the variation in the MBT$'_{5ME}$ at the site with soil warming (mean soil temperature ranging between 5 and 14 °C). At all sites, soil pH is positively related with the same brGDGTs (Ib, IIb, IIIb, IIIc, IIa$'$, IIb$'$, IIc$'$, IIIa$'$, IIb$'$, IIIc$'$) and influences the ratio between main brGDGT compounds Ia, IIa and IIIa, impacting the MBT$'_{5ME}$ values. This change in brGDGT distributions coincides with a change in the composition of the bacterial community at all sites. The bacterial clades that vary at the three experimental sites (specifically *Acidobacteria* subgroups 1, 2, 3, 6, 22) have previously been shown to also respond to soil pH on a global scale. As soil pH changes on geological timescales, the impact of changing pH on the MBT$'_{5ME}$ paleothermometer should be considered when performing paleoclimate studies.

1. INTRODUCTION

Branched glycerol dialkyl glycerol tetraethers (brGDGTs) are bacterial membrane spanning lipids with a wide structural diversity (i.e. Sinninghe Damsté et al.,

* Corresponding author at: Sonneggstrasse 5 – NO G 57, 8092 Zurich, Switzerland.

E-mail address: cindy.dejonge@erdw.ethz.ch (C. De Jonge).

2000; Weijers et al., 2006; De Jonge et al., 2013). The brGDGTs can vary in the number of methyl branches, the position of the outer methyl branch (α and/or ω-5 or 6 [5-methyl and 6-methyl brGDGTs, respectively]) and the number of internal cyclizations (0–2) (Supp. Fig. 1). On a large spatial scale, the relative distribution of 15 brGDGTs was found to vary with mean annual air temperature (MAT) and pH of soils (Weijers et al., 2007a; Peterse et al., 2012; De Jonge et al., 2014a, Naafs et al., 2017a, 2017b, Wang et al., 2019; Dearing Crampton-Flood et al., 2020). To quantify the empirical relations with respectively MAT and soil pH, the methylation of branched tetraethers (MBT$'_{5ME}$) index, and the cyclisation of branched tetraethers (CBT$'$) index were developed (Eq. (1) and (2): De Jonge et al., 2014a). Since their development, these brGDGT-based indices have been used to reconstruct temperature evolution in the Holocene (e.g. Niemann et al., 2012; Harning et al., 2020), on glacial/interglacial- (e.g. Weijers et al., 2007b; Watson et al, 2018) and on longer geological timescales (i.e. Dearing Crampton-Flood et al., 2018 [Pliocene]; Sangiorgi et al., 2018 [Miocene]; DeCelles et al., 2018 [Oligocene-Miocene]; Inglis et al., 2017; Naafs et al., 2018 [Eocene]; Super et al., 2018 [Cretaceous]). However, the bacterial producers of brGDGTs have not (yet) been identified, hampering laboratory experiments to test the empirically established relations. Until recently, the mechanism causing the environmental dependencies of the brGDGTs was assumed to be a biochemical response to changing soil pH, temperature (Weijers et al., 2007a) and moisture (Menges et al., 2014; Dang et al., 2016), needed to maintain membrane integrity. In contrast, the positive relation between the relative abundance of 6-methyl brGDGTs, quantified in the isomerization ratio (IR; De Jonge et al., 2014b), and soil alkalinity observed in global surface soils cannot be easily explained as a biochemical response (De Jonge et al., 2014a). Furthermore, Sinninghe Damsté et al. (2018) showed that the phylogenetic position of the bacterial producer might also have a possible impact on the brGDGT molecular structure. These authors observed a dependency between the occurrence and position of methylation of ether- and ester-linked iso-diabolic acid (IDA) membrane lipids (proposed brGDGTs precursors) and the phylogenetic placement of the *Acidobacteria* cultures that produced these compounds. Subsequently, a combined lipid and bacterial community study along a geothermally heated soil transect showed that the brGDGT signal only changed after passing a temperature threshold that caused a shift in the bacterial community (De Jonge et al., 2019). This implied that community change may be the mechanism underlying (part of) the variation in the MBT$'_{5ME}$ paleothermometer. Extrapolation of this community shift to the global surface soil dataset using the 'community index' (CI; Eq. (3)), revealed that brGDGTs in so-called "Cluster Cold" and "Cluster Warm" soils have a different relation with temperature and pH (De Jonge et al., 2019). Although the temperature dependency of MBT$'_{5ME}$ on a global scale can partly be attributed to changes between 'warm' and 'cold' bacterial communities, MBT$'_{5ME}$ values within "Cluster Warm" soils still correlated with MAT ($r^2 = 0.28$, $p < 0.01$). On the other

hand, while brGDGTs in mid- and high latitude soils ("Cluster Cold" soils) appeared to mainly respond to soil pH, and only to a lesser extent also to MAT, the most important chemical and/or biological driver(s) –causing 67% of the brGDGT variance in this cluster– remain(s) elusive.

To assess whether soil chemical parameters co-determine the variation in brGDGT lipids in high and mid-altitude soils (examples of Cluster Cold soils), we consider soil parameters that are known to influence brGDGTs (soil pH, soil temperature), along with additional soil chemical parameters that are known to influence bacterial communities, such as soil organic carbon (SOC) content, and soil nutrients (Ca, Mg, Mn, N, P; i.e. Wallis et al., 2010; He et al., 2012; Navarrete et al., 2013; Docherty et al., 2015; Xia et al., 2016; Pajares et al., 2016; Lynn et al., 2017). To elucidate whether membrane adaptation or bacterial community shifts determine the variation in brGDGT lipids in high and mid-altitude soils, we target and directly compare brGDGTs and bacterial communities in three well-studied sites: (i) an experimental site that has experienced long-term fertilization; the Ossekampen Experimental Site (The Netherlands, Elberse et al., 1983), (ii) a sequence of unwarmed and moderately warmed soils, part of a geothermal gradient; ForHot (Iceland, Sigurdsson et al., 2016; Walker et al., 2020) and (iii) an agricultural site where a soil pH gradient is maintained: Craibstone (Scotland, described in Kemp et al., 1992). Where changes in brGDGT distribution are observed, we identify the edaphic parameters and bacterial taxonomic orders that can be related to these changes. We then discuss the impact of our findings on the temperature proxy MBT$'_{5ME}$, both within our study sites as well as inferred implications in soils on the global scale.

2. MATERIAL AND METHODS

2.1. Study sites

The Ossekampen experimental site (hereafter: "Ossekampen") is located in the Netherlands, and is composed of a series of plots in a temperate grassland, which have been subjected to yearly additions of inorganic fertilizers since 1958 (54 years at time of sampling). In addition to a control plot, five different nutrient treatments have been performed (N, P, K, NPK and lime addition; Elberse et al., 1983). Due to the close location of the replicate plots, the same vegetation cover (grassland), and the absence of topography, no difference in soil temperature between the plots is expected. The mean annual temperature at the closest Dutch Meteorological Office (KNMI) weather station in Deelen (20 km from the Ossekampen site) is 9.7 °C [1971–2014; http://projects.knmi.nl/]. For each plot (n = 6), triplicate soil samples were taken at 0–10 cm depth (n = 18).

At Craibstone (Scotland, UK) the Woodlands Field Old rotation experiment (hereafter: "Craibstone") has established a soil pH gradient (4.5, 5.0, 5.5, 6.0, 6.5, 7.0, 7.5) by adding $Al_2(SO_4)_3$ or $Ca(OH)_2$ (lime) to podzol soils (sandy loam: Kemp et al., 1992) subjected to an agricultural

rotation scheme since 1961 (46 years at time of sampling). The mean annual temperature at the weather station "Aberdeen Airport" (1.5 km from Craibstone) is 8.1 °C [1981–2010; https://www.metoffice.gov.uk/research/climate/]. Triplicate field samples at 6 steps along the pH gradient were collected in 2006 and 2007 under potato crop (Nicol et al., 2008; Bartram et al., 2014), where the lipids were extracted from pooled soil samples collected in 2007.

The ForHot site is an Icelandic grassland where geothermal warming has resulted in a surface soil temperature transect from 5 to 25 °C over a period of at least 50 years (Sigurdsson et al., 2016). This manuscript focuses on those soils that classify as Cluster Cold soils [n = 25, Community Index (CI) values of 0.37–0.62] in a dataset previously reported by De Jonge et al. (2019).

2.2. Soil chemical analysis

The chemical characteristics of the Ossekampen site soils were previously reported in Pan et al. (2014) and Cassman et al. (2016), including total organic matter, soil moisture and available trace elements such as Al, As, Cd, Cr, Cu, Fe, Mg, Zn, Mn, Na and Ni. For the current study, samples selected for brGDGT analysis (3 samples per treatment: n = 18) were subjected to individual chemical characterization: pH was measured in 0.01 M $CaCl_2$, total Ca, K, Mg and Mn were extract with $H_2SO_4/H_2O_2/Se$ and determined using ICP-MS. Similarly, total N and P were determined with Segmented Flow Analysis (Walinga et al., 1995) [Supp. Table 1]. At the Craibstone site, chemical characteristics along the pH gradient were described in Nicol et al. (2008): water, carbon and nitrogen content (% of oven dry weight), ammonia and nitrite/nitrate were measured. Soil cations and anions have not been determined. At the ForHot site each permanent research plot has been characterized on the plot level. Total Ca, K, Mg, Mn, P and N were extracted and quantified in the same way as the Ossekampen samples (reported in De Jonge et al., 2019). The in-situ supply of soil cations in the soil solution (including, Ca, K, Mg and Mn) was measured using ion exchange resins (PRS probes, Western AG, Canada [Qian and Schoenau, 2011]) in spring and summer 2014.

2.3. Bacterial community analysis

The bacterial community composition in each treatment plot at Ossekampen (n = 6) was previously reported as an average per treatment plot by Cassman et al. (2016), following the sequencing of amplified amplicon products of the 16 rDNA V4 region, on a Roche 454 FLX Titanium platform. Here, we aim to evaluate the bacterial community data of the triplicate samples that were also used for brGDGTs quantification (n = 18). However, the operational taxonomic unit (OTU) table and taxonomic assignments of only 15 samples is available, as the plot with the K treatment was not amplified successfully. The OTU table prepared by Cassman et al. (2016) is rarefied at a depth of 1040, resulting in a total of 3207 OTUs (package "vegan" in R; Oksanen et al., 2019).

The Craibstone pH gradient was sampled in 2006 and 2007 (triplicate samples, pooled), and the V3 region of the bacterial 16S rDNA sequences was amplified to reconstruct pH-dependent bacterial community changes, as described in Bartram et al., 2014. The raw data, generated by an Illumina Miseq platform were retrieved from NCBI (accession number SRP007517) and have been re-analysed for this study. A total of 13,690 (97%) Zero-radius OTUs are encountered in the 14 samples. After rarefaction to a depth of 261,067, 13,638 OTUs remain. The dataset was narrowed down to the most abundant 90% of sequences using the package "phyloseq" in R (McMurdie and Holmes, 2013), resulting in 3572 OTUs.

For 19 out of 25 Cluster Cold ForHot soils in this study, the bacterial community has been characterized (Radujković et al., 2018; De Jonge et al., 2019). The sequences have been rarefied at a depth of 22920, resulting in a total of 7610 OTUs. Selection of the 90% most abundant sequences resulted in 2648 OTUs, that have been used for downstream analyses. Based on the similarities between in the OTU distribution of different soils at each site, Ward's minimum variance method, implementing the Ward clustering criterion (Ward, 1963), was used for clustering. We employed the package "indspecies" in R (Cáceres and Legendre, 2009) to determine those OTUs that are increased or decreased in the previously defined cluster, based on their relative abundance and their relative frequency of occurrence ("bio-indicator OTUs"). P-values were corrected using Sidak's correction for multiple testing (p < 0.05). Following up on this, the orders that were characterized by a higher number of indicator species than what is expected from random subsampling (permutation = 999, p < 0.05), were identified and are reported in bold (Supp. Table 4, 5, 6).

2.4. GDGT analysis

BrGDGTs were analyzed in triplicate samples from each Ossekampen plot (n = 18). All soil samples were stored frozen prior to freeze-drying, homogenizing, and lipid extraction using a modified Bligh and Dyer extraction (Pitcher et al., 2009). The brGDGT distribution in Craibstone soils was previously reported by Peterse et al. (2010) but does not include separated 5-methyl and 6-methyl brGDGTs. For this study, these soils collected in 2007 were re-extracted using a Milestone ETHOS X microwave extractor with a dichloromethane (DCM):Methanol (meOH) 9:1 (v/v) mixture. The brGDGTs reported for ForHot and Ossekampen were present as core lipid compounds, while Craibstone represents a mixture of core lipid and intact polar lipids. Peterse et al. (2010) reported the distribution of Craibstone IPLs (9–19% of the GDGT pool), and concluded that they follow the same response with pH as the core lipids. For both Ossekampen and Craibstone extracts a known amount of C46 GDGT standard (Huguet et al., 2006) was added to the total lipid extracts (TLE), after which TLE was eluted over an Al_2O_3 column with hexane:DCM 9:1 and DCM:MeOH 1:1 to obtain an apolar and a polar fraction, respectively. The polar fractions, containing the brGDGTs, were re-dissolved in hexane:iso-propanol 99:1

Table 1

Fractional abundance (%) and concentration of brGDGTs. BrGDGT ratios MBT′$_{5ME}$ [Eq. (1)], CBT′ [Eq. (2)], CI [Eq.3], IR [Eq. (4)], and DC′ [Eq. (5)], and reconstructed mean annual temperature (MAT [Eq. (6)]) and reconstructed pH [Eq. (7)] values for the Ossekampen and Craibstone study sites (these parameters were previously reported by De Jonge et al., 2019 for ForHot Cold Cluster soils). In addition, significant linear correlations (p < 0.05) with environmental variables pH and MAT reported, with p-value and pearson r-value indicated. This includes the Ossekampen, Craibstone and ForHot Cold Cluster datasets, as a well as for the Global Cold Cluster soils, after Sochi-based separation in High and Low pH clusters. Best correlation for each fractional abundance, ratio or reconstructed value indicated in bold.

		BrGDGTs (%)															Σ brGDGTs	BrGDGT climate ratios					Reconstructions	
		Ia	Ib	Ic	IIa	IIb	IIc	IIIa	IIIb	IIIc	IIa′	IIb′	IIc′	IIIa′	IIIb′	IIIc′	ng/g soil	MBT′$_{5ME}$	CBT′	IR	DC′	CI	MATrec	pHrec
Ossekampen																								
Control	13_1	38.4	5.0	2.4	38.1	1.9	0.3	8.3	b.d.l.	b.d.l.	4.7	0.2	b.d.l.	0.8	b.d.l.	b.d.l.	396	0.49	−1.02	0.11	0.08	0.45	6.8	3.4
	13_2	39.2	4.8	2.4	36.7	1.8	0.3	8.2	b.d.l.	b.d.l.	5.5	0.2	b.d.l.	0.8	b.d.l.	b.d.l.	263	0.50	−0.98	0.12	0.08	0.47	6.8	3.6
	13_3	39.8	4.4	2.2	37.4	1.7	0.3	8.0	0.03	b.d.l.	5.3	0.2	b.d.l.	0.7	b.d.l.	b.d.l.	356	0.49	−1.01	0.12	0.07	0.47	6.8	3.5
+ K	18_1	42.5	3.0	1.2	39.3	1.2	0.2	8.0	b.d.l.	b.d.l.	4.0	0.1	b.d.l.	0.6	b.d.l.	b.d.l.	259	0.49	−1.18	0.09	0.05	0.47	6.6	2.8
	18_2	42.6	3.0	1.5	39.4	1.2	0.2	7.9	b.d.l.	b.d.l.	3.7	0.1	b.d.l.	0.6	b.d.l.	b.d.l.	251	0.49	−1.19	0.08	0.05	0.47	6.7	2.8
	18_3	42.4	3.0	1.5	39.1	1.1	0.2	8.4	b.d.l.	b.d.l.	3.7	0.1	b.d.l.	0.6	b.d.l.	b.d.l.	266	0.49	−1.18	0.08	0.05	0.47	6.6	2.8
+ NPK	19_1	38.3	4.0	1.8	41.6	1.6	0.3	8.9	b.d.l.	b.d.l.	2.9	0.2	b.d.l.	0.4	b.d.l.	b.d.l.	278	0.46	−1.22	0.06	0.07	0.43	5.6	2.7
	19_2	39.1	4.5	2.1	39.8	1.7	0.3	8.5	b.d.l.	b.d.l.	3.2	0.2	b.d.l.	0.5	b.d.l.	b.d.l.	168	0.48	−1.16	0.07	0.07	0.45	6.2	2.9
	19_3	37.6	4.2	2.0	41.2	1.7	0.3	9.0	b.d.l.	b.d.l.	3.2	0.2	b.d.l.	0.5	b.d.l.	b.d.l.	244	0.46	−1.17	0.07	0.07	0.43	5.6	2.9
+ P	20_1	38.9	5.4	2.9	38.1	2.1	0.4	7.4	b.d.l.	b.d.l.	4.2	0.2	b.d.l.	0.6	b.d.l.	b.d.l.	237	0.50	−1.03	0.10	0.09	0.46	6.8	3.4
	20_2	39.0	5.2	2.9	37.8	2.0	0.3	7.8	b.d.l.	b.d.l.	4.0	0.2	b.d.l.	0.7	b.d.l.	b.d.l.	140	0.50	−1.03	0.09	0.08	0.46	6.8	3.4
	20_3	39.3	5.1	3.2	38.2	2.0	0.3	7.5	b.d.l.	b.d.l.	3.7	0.2	b.d.l.	0.6	b.d.l.	b.d.l.	212	0.50	−1.04	0.09	0.08	0.46	6.9	3.3
+ CaO	21_1	14.1	15.8	3.0	11.7	7.8	0.4	5.4	0.7	0.3	13.1	15.8	0.9	9.0	2.0	b.d.l.	207	0.56	0.15	0.56	0.50	0.45	8.9	7.7
	21_2	16.9	13.5	2.9	11.5	3.9	0.5	4.6	2.2	0.3	14.2	17.8	1.0	10.0	1.0	b.d.l.	109	0.62	0.15	0.60	0.45	0.51	10.6	7.7
	21_3	19.0	13.4	3.4	14.6	5.8	0.5	5.7	2.1	0.2	11.9	13.5	0.8	8.1	1.0	0.1	147	0.57	−0.01	0.50	0.42	0.48	9.2	7.1
+ N	25_1	43.0	3.0	1.3	39.4	1.2	0.2	8.3	b.d.l.	b.d.l.	2.7	0.2	b.d.l.	0.6	b.d.l.	b.d.l.	112	0.49	−1.27	0.06	0.05	0.47	6.6	2.5
	25_2	40.1	3.0	1.2	40.1	1.2	0.3	9.0	b.d.l.	b.d.l.	3.9	0.4	b.d.l.	0.8	b.d.l.	b.d.l.	114	0.47	−1.15	0.09	0.06	0.45	5.9	2.9
	25_3	43.0	3.7	2.2	37.9	1.4	0.3	8.1	b.d.l.	b.d.l.	2.8	0.2	b.d.l.	0.6	b.d.l.	b.d.l.	139	0.51	−1.19	0.07	0.06	0.48	7.1	2.8
Soil pH	r	−0.98	0.97	**0.61**	−0.98	**0.89**	0.81	−0.93	0.92	0.98	0.98	0.98	0.98	0.98	**0.89**	0.53		0.91	0.99	0.99	0.98	n.d.	0.91	0.99
	p	<0.01	<0.01	<0.01	<0.01	<0.01	<0.01	<0.01	<0.01	<0.01	<0.01	<0.01	<0.01	<0.01	<0.01	<0.05		<0.01	<0.01	<0.01	<0.01	n.d.	<0.01	<0.01
Craibstone																								
pH plot	4.5	42.2	3.1	0.8	39.5	1.2	0.3	8.1	b.d.l.	b.d.l.	3.7	0.4	0.03	0.7	b.d.l.	b.d.l.	2112	0.48	−1.21	0.08	0.05	0.47	6.66	5.23
	5	44.0	3.0	0.8	37.7	1.3	0.3	7.6	b.d.l.	b.d.l.	4.2	0.4	0.03	0.8	b.d.l.	b.d.l.	1837	0.51	−1.16	0.1	0.05	0.49	7.33	5.31
	5.5	43.2	3.2	1.0	35.3	1.4	0.3	6.7	b.d.l.	b.d.l.	6.9	0.5	0.03	1.5	b.d.l.	b.d.l.	1764	0.52	−0.93	0.17	0.06	0.51	7.81	5.67
	6	39.9	5.1	1.5	31.2	2.5	0.4	6.3	b.d.l.	b.d.l.	9.6	1.4	0.06	2.3	b.d.l.	b.d.l.	1993	0.54	−0.72	0.24	0.1	0.52	8.26	6.01
	6.5	37.3	6.9	1.7	25.9	3.8	0.4	5.7	0.1	0.04	11.5	2.9	0.1	3.4	0.2	0.05	1589	0.56	−0.54	0.32	0.15	0.54	9.1	6.29
	7	35.3	7.5	1.9	23.0	4.0	0.4	5.6	0.2	0.05	12.4	4.2	0.2	4.8	0.4	0.09	1519	0.57	−0.43	0.37	0.18	0.55	9.51	6.47
	7.5	34.6	6.9	1.7	20.4	3.9	0.5	5.4	0.2	0.05	12.5	6.0	0.3	6.7	0.9	0.2	1176	0.59	−0.33	0.43	0.2	0.57	9.95	6.62
Soil pH	r	−0.93	0.94	0.95	−0.99	0.96	0.96	−0.98	0.89	0.89	0.99	0.91	0.92	0.94	0.81	0.84	−1	1	1	0.99	0.96	n.d.	1	1
	p	<0.01	<0.01	<0.01	<0.01	<0.01	<0.01	<0.01	<0.01	<0.01	<0.01	<0.01	<0.01	<0.01	<0.05	<0.05	<0.01	<0.01	<0.01	<0.01	<0.01	n.d.	<0.01	<0.01
ForHot – Cold Cluster soils																								
Soil pH	r	−0.69	0.80		−0.72	0.79	0.73	−0.40	0.73	0.63	0.73	0.72	0.79	0.43	0.66	0.60			0.73	0.75	0.77			0.73
	p	<0.01	<0.01		<0.01	<0.01	<0.01	0.05	<0.01	<0.01	<0.01	<0.01	<0.01	0.03	<0.01	<0.01			<0.01	<0.01	<0.01			<0.01
MAT	r							**−0.53**																
	p							**<0.01**																

and filtered over a 0.45 um PTFE filter, prior to injection on an Agilent 1260 HPLC coupled to an Agilent 6130 single quadrupole mass detector following the chromatographic method of Hopmans et al., 2016. The 15 brGDGT lipids are represented as absolute and fractional abundances (FA) in Table 1 [Ossekampen and Craibstone] and in De Jonge et al. (2019) [ForHot]. The brGDGT distribution can be further summarized as brGDGT ratios that have been shown to correlate with bacterial community composition (CI: De Jonge et al., 2019) or with environmental parameters on a global scale, so-called climate proxies (De Jonge et al., 2014a, Yang et al., 2015). The climate proxies summarize the degree of branching of 5-methyl GDGTs (MBT′$_{5ME}$), inclusion of cyclopentane moieties (CBT′) and the relative abundance of 6-methyl versus 5-methyl brGDGTs (IR). The annotation of the DC′ (degree of cyclization) specifically includes the 5 and 6-methyl brGDGTs compounds that were also included in the DC as formulated by Sinninghe Damsté et al. (2009). The transfer functions that are used to reconstruct MAT and soil pH based on MBT′$_{5ME}$ and CBT′ ratio values are calculated according to De Jonge et al. (2014a).

$$MBT'_{5ME} = \frac{(Ia + Ib + Ic)}{(Ia + Ib + Ic + IIa + IIb + IIc + IIIa)} \quad (1)$$

$$CBT' = {}^{10}\log\left[\frac{(Ic + IIa' + IIb' + IIc' + IIIa' + IIIb' + IIIc')}{(Ia + IIa + IIIa)}\right] \quad (2)$$

$$CI = \frac{Ia}{(Ia + IIa + IIIa)} \quad (3)$$

$$IR = \frac{(IIa' + IIIa')}{(IIa + IIIa + IIa' + IIIa')} \quad (4)$$

$$DC' = \frac{(Ib + IIb + IIb')}{(Ia + IIa + IIa' + Ib + IIb + IIb')} \quad (5)$$

$$MAT = -8.57 + 31.45 * MBT'_{5ME} \quad (6)$$

$$pH = 7.15 + 1.59 * CBT' \quad (7)$$

BrGDGT fractional abundances and their significant linear correlations ($p < 0.05$) with measured environmental parameters are reported [pearson r-value] in Table 1, as well as brGDGT concentrations. BrGDGT concentrations of ForHot soils have not been published previously and are reported in Supp. Table 2. BrGDGT ratios [Eqs. (1)–(5)] and reconstructed pH and MAT values [Eqs. (6) and (7)] are reported in Table 1. The correlations between values of environmental variables and site loadings on the principal components are reported in Supp. Table 3 [pearson r-value]. To determine whether the brGDGT fractional abundances and ratio values between the different treatments at the Ossekampen site are significantly different, an ANOVA was computed with the 'Tukey Honest Significant Differences' method. To summarize the variability in brGDGT distributions, a principal component analysis (PCA) was performed on scaled brGDGT abundances. Compounds that are often below detection limit were excluded from this analysis (specifically, brGDGT IIIc′ in the Ossekampen dataset). Environmental parameters are plotted *a posteriori*

in the ordination space. These analyses were performed in R, using the package "stats" and "vegan" (R Core Team, 2018; Oksanen et al., 2019).

3. RESULTS

3.1. Ossekampen

At the Ossekampen experimental site, the plots are characterized by a large inter-plot chemical variability, corresponding to the different treatments. This results in soil pH values varying from 4.0 to 6.8, and large variations in extractable Ca (2600–11,000 mg*kg^{-1} dry soil), K (7700–12,000 mg*kg^{-1} dry soil), Mg (6474–7349 mg*kg^{-1} dry soil), Mn (213–386 mg*kg^{-1} dry soil), P (700–1490 mg*kg^{-1} dry soil) and N (4957–7283 mg*kg^{-1} dry soil) (Supp. Table 1). N-NH$_4$: (2.7–14.8 mg*kg^{-1} dry soil) and N-(NO$_{NO2}$): (1.4–15.8 mg*kg^{-1} dry soil) have been determined on plot level (Pan et al., 2014; Cassman et al., 2016). The percentage of organic matter is comparable between plots (14.3–15.6%), where slightly increased values are associated with the CaO treated ("limed") plot. In the limed plot, soil pH (6.5–6.8) is higher compared to the other plots (4.0–4.5; Supp. Table 1).

The concentration of brGDGT lipids (ng*g^{-1} soil) is higher in the untreated plot ("Control": 260–400 ng*g^{-1} soil) than in the treatment plots (Fig. 1A). While the K and NPK treated plots show a lower brGDGT concentration (170–280 ng*g^{-1} soil), the plots with P, N and liming treatments have significantly decreased abundances (110–240 ng*g^{-1} soil, [$p < 0.05$]), compared to the control plot. The change in concentration of individual brGDGTs (Supp. Fig. 2) shows that the major 5-methyl brGDGTs Ia, IIa and IIIa mirror the pattern in the abundance of total brGDGTs, with significantly ($p < 0.05$) decreased concentrations in the N, P treated and limed soils (Ia additionally decreased in NPK treated soil), compared to the control soil. On the other hand, the concentration of 6-methyl brGDGT IIa′ does not drop in the limed soils, while brGDGT IIIa′ even shows an increased concentration in these soils (Fig. 1B). Also, several cyclopentane-containing brGDGTs show a conserved (Ib, Ic, IIb, IIc), or even an increased concentration (i.e. Ib, IIb, IIIb, IIIc, IIb, IIc′, IIIb′, IIIc′) in limed soils (Supp. Fig. 2), compared to the control soil. Principal component analysis of the brGDGT fractional abundances indicates that pH is the abiotic factor that explains most of the variation (Fig. 1C; Supp. Table 3), and fractional abundances of brGDGTs that have high loading on the PC1 (Ia, Ib, IIa, IIb, IIc, IIIa, IIIb, IIIc, IIa′, IIb′, IIc′, IIIa′, IIIb′, IIIc) show strong linear correlations (absolute r values between 0.89 and 0.98 [Table 1]) with soil pH. Those compounds that show a high loading on PC2 show a less strong dependency with soil pH: Ic and IIc ($r = 0.61$ and 0.81 [Table 1]).

The fractional abundance of the 15 brGDGT compounds is used to calculate the CBT′, DC′ and MBT′$_{5ME}$ (Fig. 1D–F). CBT′ index values [−2.93 to 0.35] are significantly different ($p < 0.001$) between the control and P addition plots (a), the N, K and NPK addition plots (b) and again different from the limed soils (c; Fig. 1D). IR
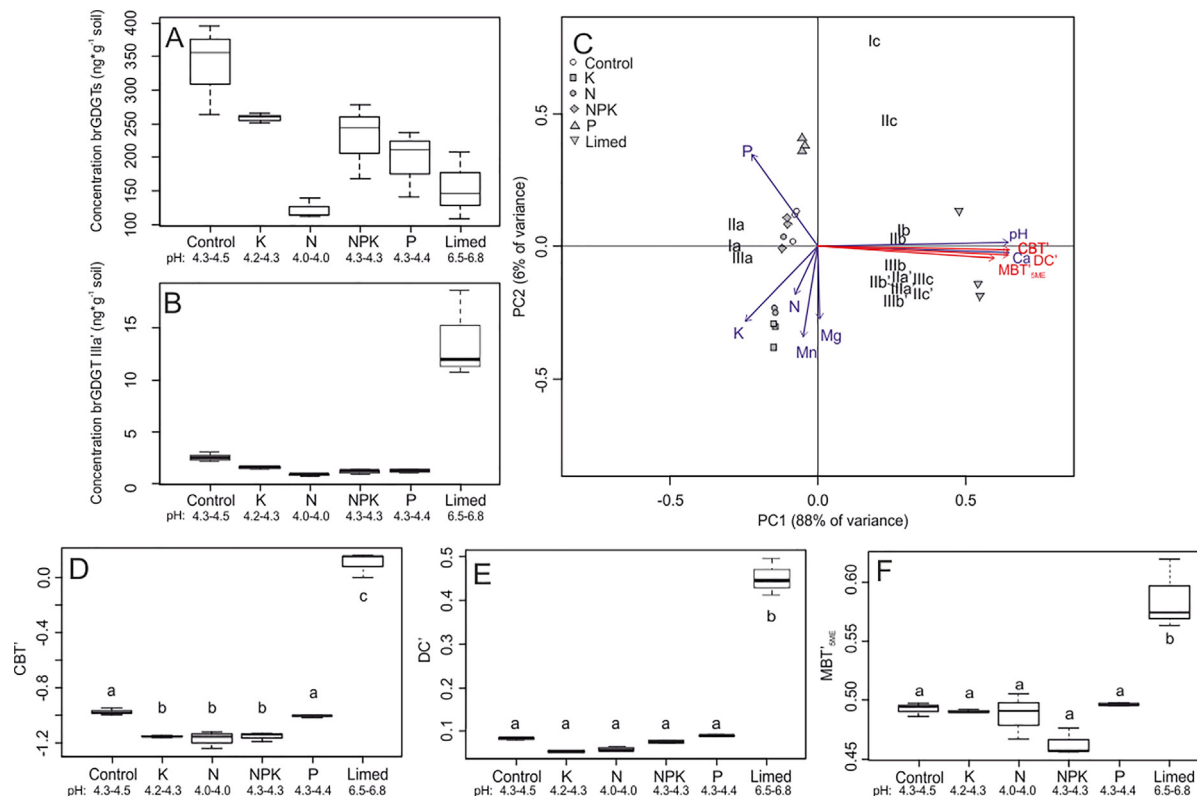
Fig. 1. Ossekampen soils –concentration of (A) all brGDGTs and (B) brGDGT IIIa′, boxplot based on triplicate measurement for each treatment, range of measured soil pH values indicated. (C) An unconstrained PCA based on the standardized fractional abundances of 14 brGDGT compounds, with loading of the brGDGT compounds and sites plotted in the ordination space. Environmental factors are plotted *a posteriori*, the vector IR has been ommitted to avoid overlap with MBT′$_{5ME}$. BrGDGT-based ratios CBT′ values (D [Eq. (2)]), DC′ (E [Eq. (5)]) and MBT′$_{5ME}$ (F [Eq. (1)]), values for each treatment (triplicate). Measured soil pH values indicated below each treatment. Different letters indicate groups with statistically different averages.

ratio values follow the same environmental distribution as the CBT′ values (r = 0.99, p < 0.01). The DC′ values vary between 0.05 and 0.50, with significantly different values between (a) the control, N, K, NPK and P addition plots and (b) the limed plot (Fig. 1D). The MBT′$_{5ME}$ index values [0.46–0.62] vary significantly (p < 0.05) between the limed soils (a) and all other treatments (b) (Fig. 1F). The increased MBT′$_{5ME}$ values in the limed soils result in reconstructed temperatures between 8.9 and 10.6 °C, compared to values between 5.6 and 7.1 °C in other treatments and control plots. Both the values of the CBT′ index (r = 0.99, p < 0.01, n = 18), the DC′ index (r = 0.98, p < 0.01, n = 18), the IR ratio (r = 0.99, p < 0.01, n = 18) and the MBT′$_{5ME}$ correlate with soil pH (r = 0.91, p < 0.01, n = 18). BrGDGT distributions result in CI values between 0.10 and 0.43 (Table 1). All soils thus fall within the Cluster Cold based on the threshold of 0.64 set by De Jonge et al. (2019).

The treatment-dependent OTU distribution in the Ossekampen soils have been reported by Cassman et al. (2016). A cluster analysis of the bacterial community composition (Fig. 2A) shows that the 3 samples from the limed soil have a different composition and plot separate. Using a bio-indicator approach for both clusters, 139 OTUs are identified as bio-indicators, showing increased abundances

in high pH (limed) soils (7% of all OTUs), and 53 OTUs as bio-indicators, showing increased abundances in low pH soils (2% of all OTUs). Their phylogenetic spread is reported in Supp. Table 4.

3.2. Craibstone

At the Craibstone experimental site an artificial pH gradient is maintained, where the pH is either lowered by addition of $Al_2(SO_4)_3$ or increased by addition of $Ca(OH)_2$. Soils collected in 2006 have a pH range of 4.9–7.5. Samples collected in 2007, from a parallel plot, generally have somewhat lower pH values of 7.28 [7.5], 7.04 [7.0], 6.63 [6.5], 6.00 [6.0], 5.50 [5.5], 4.92 [5.0] and 4.43 [4.5] (sample name between brackets). Nicol et al. (2008) report that neither the average carbon (6.4–8.0% dry weight), soil moisture (29–31% dry weight), nitrogen (0.29–0.40% dry weight), nor ammonia (1.4–1.7 µg*g^{-1} soil) shows a significant correlation with soil pH in the soils. Only the nitrate/nitrite concentrations (all soils: 9.5–15.1 µg*g^{-1} soil [NO_2^-/NO_3^- N]) have increased values in low pH soils (pH = 4.9 and 5.3, 15.1–15.0 µg*g^{-1} soil [NO_2^-/NO_3^- N]).

The summed concentration of brGDGTs (380–660 ng*g^{-1} soil) decreases with increasing soil pH (Table 1, Fig. 3A). However, not all brGDGT compounds respond in
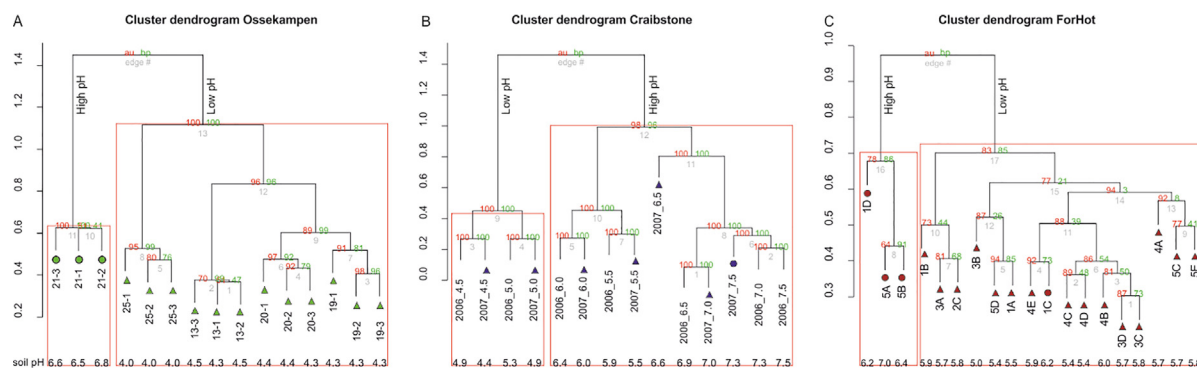
Fig. 2. Cluster dendrogram based on the rarefied OTU tables with AU (red) and BP (green) % values of the (A) Ossenkampen, (B) Craibstone soils and (C) ForHot soils, with high pH and low pH clusters indicated. Soils with CBT′ < −0.37 are indicated with a triangle, soils with CBT′ > −0.37 are indicated with a circle. (For interpretation of the references to colour in this figure legend, the reader is referred to the web version of this article.)
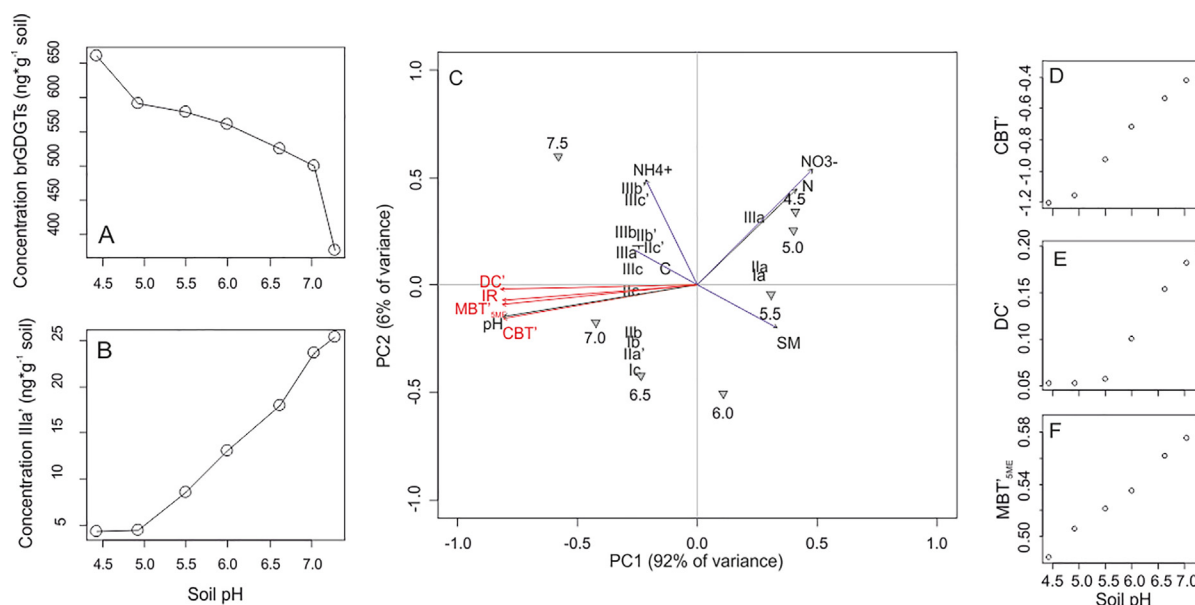
Fig. 3. Craibstone soils – concentrations of (A) all brGDGTs and (B) brGDGT IIIa′. (C) An unconstrained PCA based on the standardized fractional abundances of 15 brGDGT compounds, with the loading of the brGDGT compounds and sites (triangle with site name) plotted in the ordination space. Environmental factors are plotted a posteriori. (D–F) brGDGT ratios CBT′ [Eq. (2)], DC′ [Eq. (5)] and MBT′$_{5ME}$ [Eq. (1)] values plotted against measured soil pH.

the same way. While the concentrations of non-cyclopentane containing 5-methyl brGDGTs Ia, IIa and IIIa decrease with soil pH, the other brGDGTs show an increase with soil pH. BrGDGTs IIa′ and IIIa′ start increasing at a pH > 5.0 (Fig. 3B, Supp. Fig. 3), while cyclopentane-containing brGDGTs only increase at soil pH of 6.0 (Ib, Ic, IIb, IIc, IIb′, IIc′) or 6.5 (IIIb, IIIc, IIIb′, IIIc′). The 5-methyl compounds (brGDGT Ib, Ic, IIb, IIc, IIIb, IIIc) that increase in concentration with pH show a maximum at pH 6.6–7.0. The 6-methyl brGDGTs however (with the exception of IIa′) generally show an increased concentration even in soils with a pH of 7.3 (Supp. Fig. 3).

The fractional abundance of the brGDGT compounds also show a strong correlation with measured pH. Similar to Peterse et al. (2010) we observe a decrease of the fractional abundance of brGDGTs Ia, IIa and IIIa with increasing pH (r = −0.95, −1.0, −0.96, respectively, p < 0.01: Table 1). The remaining brGDGTs show a contrasting response, increasing with increased pH (r = 0. 85–0.97, p < 0.01). The PCA shows that pH correlates well with the site scores on PC1 (r^2 = 0.92, p < 0.001, Fig. 3C, Supp. Table 3). BrGDGT ratios show a strong correlation with the soil pH values (CBT′ range: −0.3 to 0.01, r = 0.99, p < 0.01, n = 7 [Fig. 3D]; IR range: 0.08–0.43, r = 0.99, p < 0.01, n = 7; DC′ range: 0.05–0.20, r = 0.96, p < 0.01, n = 7, [Fig. 3E]). A novel observation is that also the MBT′$_{5ME}$ (range: 0.48–0.59: Table 1) correlates strongly with the soil pH (r = 1.00, p < 0.01, n = 7 [Fig. 3F]).

The bacterial community at Craibstone was previously shown to strongly respond to soil pH (Bartram et al.,
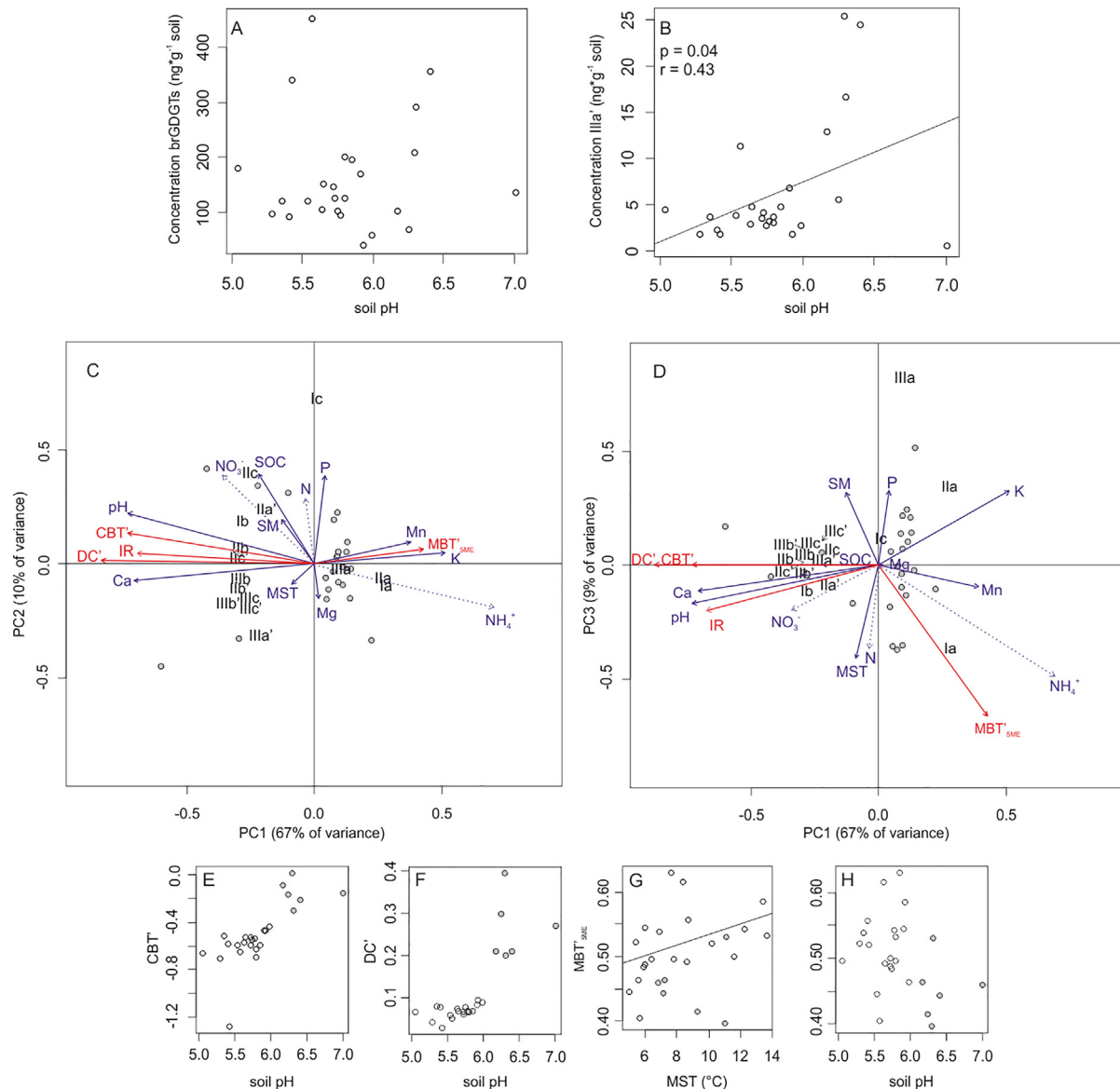
Fig. 4. ForHot Cold Cluster soils – concentrations of (A) all brGDGTs and (B) brGDGT IIIa′. (C–D) An unconstrained PCA based on the standardized fractional abundances of 15 brGDGT compounds, with the loading of the brGDGT compounds and sites plotted in the ordination space. Environmental factors and brGDGT ratios are plotted *a posteriori*. E) CBT′ [Eq. (2)] and F) DC′ [Eq. (5)] values plotted against soil pH, G-H) MBT′$_{5ME}$ [Eq. (1)] values plotted versus soil pH and mean annual soil temperature (MST). Those soils with a CBT′ value > −0.37 are indicated in with grey symbols in panels E-F. In panel G, the significant correlation between low pH soils (white symbols) and MST is plotted.

2014). Applying a clustering method reveals two clusters, with low pH soils (pH between 4.4 and 5.3) contrasted against soils with medium and high pH values (pH > 5.3; Fig. 2B). 1586 taxa are identified as bio-indicators for high pH soils (44% of all OTUs) and 487 OTUs are identified as bio-indicators for low pH soils (14% of OTUs).

3.3. ForHot

Along the ForHot geothermal gradient (De Jonge et al., 2019), the 25 soils selected have in-situ measured Mean Soil Temperature (MST) between 5.0 and 13.7 °C. The organic

carbon content varies between 1 and 8% (Leblans, 2016), decreasing with increasing MST ($r^2 = 0.49$, $p < 0.01$, $n = 25$). Soil pH varies between 5.1 and 7.0 and does not correlate with the MST ($r = 0.16$, $p > 0.4$, $n = 25$). Soil nutrients (total P [640–1670 mg*kg^{-1} dry soil]) and total Ca [5580–17,820 mg*kg^{-1} dry soil], Mg [7570–22,010 mg*kg^{-1} dry soil], Mn [1140–2030 mg*kg^{-1} dry soil], K [up to 1420 mg*kg^{-1} dry soil] and available concentrations (spring, summer) of the cations K (8–330 µg*10 c m^{-2}*89 days^{-1}), Mg (110–440 µg*10 cm^{-2}*89 days^{-1}), and Ca (250–2500 µg*10 cm^{-2}*89 days^{-1}) have been determined (Supp. Fig. 4). Of these, soil pH correlates with total

Ca (r = 0.66, p < 0.05, n = 25), total Mn (r = −0.42, p < 0.05, n = 25) and total K (r = −0.42, p < 0.05, n = 25). Significant correlations between MST and the soil cations are plotted in Supp. Fig. 4. No correlation between the summed concentration of brGDGT lipids (40–450 ng*g^{-1} soil) and soil pH is observed (Fig. 4A). The amount of brGDGT Ia and IIa is higher in soils with pH < 6.1 (mean = 61 and 48 ng*g soil^{-1}, respectively) compared to soils with pH > 6.1 (mean = 37 and 29 ng*g soil^{-1}, respectively), although no linear correlation is present. A significant correlation is present between soil pH and the concentration of brGDGTs IIa′ (r = 0.40, p < 0.05, n = 25) and IIIa′ (r = 0.42, p < 0.05, n = 25) [Fig. 4B, Supp. Fig. 5]. Furthermore, the individual concentrations of the cyclopentane containing brGDGTs (with the exception of Ic) show a significant increase with soil pH (0.54 < r < 0. 72, p < 0.05). For several compounds (Ib, IIb, IIc, IIIb, IIIc, IIb′, IIc′, IIIb′, IIIc′), this increase is present only when a pH threshold of ~6.1 is crossed (Supp. Fig. 5). The PCA of the ForHot soils shows the driving effect of soil pH on the brGDGTs fractional abundances (Fig. 4C, Supp. Table 3). Soil pH correlates significantly with the fractional abundance of most brGDGTs (0.43< |r| <0.8, p < 0.05), except for brGDGT Ic and IIIa (Table 1). The CBT′ values (Fig. 4E), varying between −0.3 and 0.1, correlate with soil pH (r = 0.73, p < 0.01, n = 25), as well as the IR values (range = 0.75, p < 0.01, n = 25) and the DC′ values (r = 0.77, p < 0.01, n = 25, Fig. 4F). The MBT′$_{5ME}$ values (Fig. 4G, H) vary between 0.40–0.63 and do not correlate with soil pH (r = −0.32, p = 0.12, n = 25) or soil temperature (r = 0.27, p = 0.19, n = 25).

At the ForHot site the cluster analysis, based on a bacterial community composition, shows that the community in soils with pH > 6.1 is distinct from ForHot soils with pH < 6.1 (Fig. 2C), except for one soil where the pH measured on the soil sample used for lipid extraction was equal to 6.2. However, at this site the pH on the plot level measured in 2014 (average of 3 samples) was only 5.8 (Sigurdsson et al., 2016). The spatial variability of the soil pH within this plot probably caused the sample collected for the bacterial 16S rDNA sequence profiling to contain a community adapted to a lower pH environment, compared to the sample used for the lipid extraction, on which the higher pH of 6.2 was measured. Using a bio-indicator approach, 358 OTUs are identified as bio-indicator OTUs that increase in high pH (pH > 6.1) plots (14% of all OTUs) and 142 OTUs that increase in low pH plots (5% of all OTUs).

4. DISCUSSION

4.1. Effect of soil chemistry and temperature on brGDGT distributions

At the Ossekampen and Craibstone sites there is no variation in environmental parameters among the different soils, so all changes in brGDGT distributions can be attributed directly to changes in the soil chemistry. To distinguish between a temperature and pH effect on brGDGT concentrations and distributions, we study the ForHot study site, where both soil pH and soil temperature vary independently. At all sites, summed brGDGT concentrations are generally higher in low pH soils (Figs. 1A, 3A, 4A), reflecting a higher production or conservation of brGDGT lipids in these soils. Not all brGDGT compounds show the same variation. While the concentrations of brGDGTs Ia, IIa and IIIa are higher in low pH soils, all other brGDGTs (Ib, Ic, IIb, IIc, IIIb, IIIc, IIa′, IIb′, IIc′, IIIa′, IIIb′, IIIc′) are generally increased at high soil pH (Supp. Figs. 2, 3, 5), without following a linear trend. The distinct trends between the brGDGT concentrations indicates that degradation of brGDGTs in high pH soils is not the cause for the decreased total concentration. Instead, there is preferential production of different brGDGT lipids under low pH and high pH conditions. At Ossekampen, the pH gradient has a low resolution (soil pH increases in large increment). Here, this change happens at a poorly defined pH (between 4.5 and 6.5). At Craibstone, a pH gradient at higher resolution (soil pH changes in small increments) allows to discern two different pH responses: non-cyclopentane containing 6-methyl brGDGTs start to increase at pH > 5.0, whereas cyclopentane-containing 5-methyl (CP 5-methyl) and cyclopentane-containing 6-methyl brGDGTs (CP 6-methyl) only increase at pH > 5.5. The concentration of CP 5-methyl brGDGTs increases with soil pH, but decreases again at pH > 7.3. 6-methyl brGDGT concentrations on the other hand are highest in the soil with pH = 7.3 (Supp. Fig. 3). At ForHot, with a high resolution pH gradient, a very sharp pH threshold (pH = 6.1) is present above which the concentrations of all alkalinity-promoted compounds increase (Supp. Fig. 5).

The variation in fractional abundances is related to the change in brGDGT concentration with soil pH. The PCA of brGDGT distributions at Ossekampen, ForHot and Craibstone (Figs. 1C, 3C, 4C) reveals that the majority of variation in brGDGT compounds captured by PC1 correlates with soil pH and calcium (Supp. Table 3). Compounds with a positive relation with soil pH at the three sites are brGDGT Ib, IIb, IIIb, IIIc, IIa′, IIb′, IIc′, IIIa′, IIIb′, and IIIc′, which will from now on be referred to as "alkalinity-promoted" compounds. This trend with pH was already observed by Weijers et al. (2007a) in the first dataset of globally distributed soils, and later confirmed by Peterse et al. (2010), but was not consistently present over smaller pH ranges (pH 6.8–8.6; Dang et al., 2016). The PCAs of Ossekampen, Craibstone and ForHot also reveal that an unknown environmental factor influences brGDGT Ic (and brGDGT IIc at Ossekampen and ForHot), which shows a high loading on the second PC at the three sites (Figs. 1C, 3C, 4C: Supp. Table 3). At the Ossekampen site, the concentration of brGDGT Ic is significantly lower in the plots that have been treated with NPK and K. The fractional abundance of brGDGT Ic correlates significantly with the concentration of extractable K (r = −0.61, p < 0.01), and not with the concentration of P, Mg or Mn, that also plot along the second PC. At the Craibstone site, the concentration of brGDGT Ic reaches a maximum in soils with pH of 6.6 and 7.0 (Supp. Fig. 3). These soils have the highest potential autotrophic nitrification rates at Craibstone (Killham, 1990; Nicol

et al., 2008), suggesting a possible link between brGDGT Ic (Ib, IIa′ and IIb to a lesser extent) and the occurrence of ammonia oxidizing bacteria (AOB) and nitrite oxidizing bacteria (NOB) (Nicol et al., 2008). There is however no increase in the concentration or fractional abundance of brGDGT Ic in the Ossekampen NPK plot, although *Nitrospira*, a clade that contains autotrophic NOB, was increased under this treatment (Cassman et al., 2016). At ForHot, the PCA indicates that brGDGTs Ic is produced mainly in higher nutrient and high organic matter soils (Fig. 4C), which would support bacterial nitrification (AOB and NOB), although neither N species, total P or SOC content correlate significantly with the fractional abundance of brGDGT Ic (p > 0.05). Although all links with environmental drivers are tentative at this point, brGDGT Ic clearly shows variability that is not caused by a change in either pH or temperature. It is, however, a compound that is part of the temperature proxy MBT′$_{5ME}$, and its inclusion is crucial in obtaining a good relation with MAT (Peterse et al., 2012; De Jonge et al., 2014a). At the ForHot sites, where a 9 °C temperature gradient is present, MST only has a small loading on PC1 and PC2 and thus does not correlate with the main sources of variation (Supp. Table 3). Instead, the MST ($r^2 = 0.16$, $p < 0.05$, Supp. Table 3) correlates best with the third PC (9% of variance explained [Fig. 4D]). The brGDGT loadings on this PC show the decrease of brGDGT IIIa (and increase of brGDGT IIa and Ia) with increasing temperature. Only the fractional abundance of brGDGT IIIa correlates significantly with the MST (Table 1, De Jonge et al., 2019).

Our local scale studies confirm the positive correlation between pH (and/or Ca) and CP containing 5-methyl compounds (Ib, IIb, IIIb, IIIc) and 6-methyl compounds (IIa′, IIb′, IIc′, IIIa′, IIIb′, IIIc′) that also found on a global scale (De Jonge et al., 2019), but additionally reveal the presence of a site-specific pH threshold value (between 5.0 and 6.5) that affects the concentration and fractional abundance of alkalinity-promoted compounds at the different study sites (Supp. Figs. 2, 3, 5). As a crude assignment, high concentrations of brGDGTs Ia and IIa are characteristic for low pH environments, CP 5-methyl brGDGTs show highest concentrations in soils at intermediate pH values (6.0–7.0), while 6-methyl brGDGTs increase in concentration in intermediate and high pH soils (6.0–7.5) [Supp. Figs. 3, 5].

4.2. Effect of soil pH on the microbial community

Recently, a step-wise change in the composition of brGDGTs lipids across a temperature threshold was shown to be related to a dramatic shift in the bacterial community present in the same soils (De Jonge et al., 2019). Soil pH is also known to influence the bacterial community both on local and global scales (Fierer and Jackson, 2006; Lauber et al., 2009; Fierer et al., 2012; Ramirez et al., 2014; Delgado-Baquerizo et al., 2018). To determine whether a changing bacterial community can explain the observed shift in brGDGT concentration and fractional abundance across the pH thresholds in the Ossekampen, Craibstone and ForHot sites, we assess the pH relation of the bacterial community composition at each site. Following a clustering

approach, we find indeed that the microbial community changes at a certain soil pH (Fig. 2A–C). At the Ossekampen site this happens across a less precise defined pH threshold (between 4.5 and pH 6.5), at the Craibstone site as pH changes from 5.3 to 5.5, in ForHot soils the community changes as pH changes between 6.0 and 6.2. This bacterial 16S rDNA sequence-based clustering matches with the pH thresholds based on the changes in brGDGT signals in the same soils, thus indicating a possible influence of the bacterial community composition on the brGDGT distribution (Fig. 2). To determine which bacterial community change is related to the change in soil pH at each site, the phylogenetic placement of those OTUs that increase in the low and high pH soils is determined using a bio-indicator approach. Comparing the resulting phylogenetic groupings of these OTUs at the Ossekampen, Craibstone and ForHot sites indicates that there is no conserved response to the increase in pH on the phylum taxonomic level (Supp. Table 4, 5, 6). On lower taxonomic levels (class – order – family), however, there are a number of clades that show a conserved response in high pH soils between sites (Supp. Table 4, 5, 6; order level: Supp. Fig. 6).

As proposed brGDGT precursor compounds (i.e. iso-diabolic acid [IDA]) have so far been found uniquely in *Acidobacteria* cultures (Sinninghe Damsté et al., 2018), we specifically focus on phylogenetic changes within the phylum *Acidobacteria*. Specifically, within the phylum of *Acidobacteria* (Fig. 5), subgroup 6 is significantly increased at all 3 sites in high pH soils ($p < 0.01$), and subgroup 22 is increased significantly both at Craibstone and Ossekampen ($p < 0.05$). Subgroup 18 and subgroup 4 contain bio-indicator OTUs at all sites, and are significantly increased at one site (Ossekampen and Craibstone, respectively, $p < 0.05$). The dominant effect of soil pH on *Acidobacteria* is well-documented (Jones et al., 2009; Kielak et al., 2016), with the abundance of subgroups 4, 6, 7, 10, 11, 11, 16, 17, 18, 22, 25 increasing in soils with increased pH (reviewed in Kielak et al, 2016). Besides a direct effect of soil pH, other cations have been inferred to explain variation in *Acidobacteria* subgroups. For example, Navarrete et al. (2013) showed that subgroup 6 increased with increasing Ca, Mg, Mn and B content in Amazonian soils. With Mg and Mn constant across the pH gradient at Ossekampen (Supp. Table 1), the increase of subgroup 6 can thus be a direct effect of the addition of Ca. At Craibstone, Ca is added to increase the pH in high pH soils, where subgroup 6 is seen to increase. At the ForHot site, where pH is not manipulated, Ca concentrations are naturally higher in high pH soils (Supp. Fig. 4), and can thus again explain the increasing relative abundance of subgroup 6. The low pH soil clusters also contain a phylogenetically large range of bio-indicator OTUs. Again, on the phylum level there is no conserved response between sites. More agreement between the different sites is seen on a lower taxonomic level (Supp. Fig. 6, Supp. Table 4, 5, 6). Within the *Acidobacteria* (Fig. 5), low pH soil clusters show a consistent increase of *Acidobacteria* subgroups 1, 2 and 3. Cultured members of the *Acidobacteria* subgroups 1 and 3 have pH growth optima below 6.5 (Kuramae and Costa, 2019), and the abundance of subgroup 1, 2, 3, 12, 13 and 15 was shown
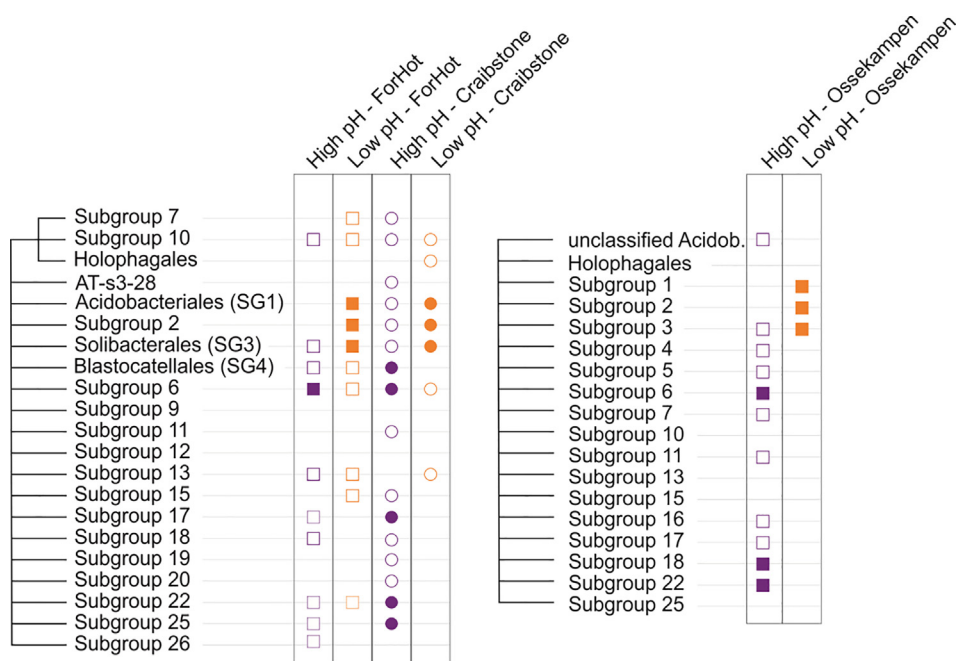
Fig. 5. Phylogenetic spread of Acidobacterial bio-indicator OTUs at Craibstone, ForHot and Ossekampen High pH and low pH soils (Fig. 3). Empty symbols indicate that bio-indicator OTUs for high pH soils (purple) or low pH soils (orange) are present within the clade. Filled symbols indicate that the clade is significantly enriched in bio-indicator OTUs. An extended phylogenetic analysis (order level) is presented in Supp. Fig. 6. (For interpretation of the references to colour in this figure legend, the reader is referred to the web version of this article.)

to anti-correlate with soil pH on global and local scales (subgroup 1: Jones et al., 2009, Costa et al.; 2020; subgroups 1–3: Rousk et al., 2010; Bartram et al., 2014, reviewed in Kielak et al., 2016).

Proposed brGDGT building blocks (IDA and mono-glycerol ether-bound IDA: IDA-MGE) have only been found within *Acidobacteria* cultures from subgroups 1, 3, 4 and 6 (Sinninghe Damsté et al., 2011; 2014; 2018). Our analyses along pH gradients show that of these, *Acidobacteria* subgroups 1 and 3 are indicative of low pH and subgroup 4 and 6 of high soil pH conditions. A methylated precursor of 6-methyl brGDGTs (6-methyl IDA) was found in all available cultures (n = 2) from *Acidobacteria* subgroup 6 (1–14% of fatty acids and ether lipids, relative abundance), and in lower amounts in some cultures (3 out of 10) of subgroup 1 and 3 (0–3%). Here, especially subgroup 6 increases in the high pH soils (possibly driven by Ca), and we propose that they are suspected producers of 6-methyl brGDGTs in the environment. Subgroup 1 and 3, that produce no, or only small amounts of 6-methyl brGDGT precursors, are indicative of low pH soils, where the fractional abundance of 6-methyl brGDGTs is low (4–25%). In these soils, they can be expected to contribute to the production of brGDGT Ia, as their lipid profile in culture is mainly composed of IDA without additional branches (Sinninghe Damsté et al., 2018). An IDA-MGE with an additional branch on the C5 position (5-methyl IDA-MGE), a possible precursor of the 5-methyl penta- and hexamethylated brGDGTs, is currently only recovered from cultured representatives from subgroup 4 (Sinninghe

Damsté et al., 2018). *Acidobacteria* subgroup 4 contains OTUs that increase in high pH soils. If we expect them to contribute to brGDGT production in high pH soils, *Acidobacteria* subgroup 4 could be the source of 5-methyl brGDGTs with internal cyclizations, as brGDGTs IIa and IIIa have an affinity for low pH soils. There is thus a possible match between the presence of 5- and 6-methyl precursor lipids in *Acidobacteria* cultures (i.e. Sinninghe Damsté et al., 2018) and the pH dependency of Acidobacterial subgroups and brGDGT lipids in the environment. This supports the proposed role of *Acidobacteria* as producer of brGDGTs in soils.

Following up on the absence of substantial amounts of complete brGDGTs in *Acidobacteria* cultures, Sinninghe Damsté et al. (2018) mapped the *elbB – elbE* gene cluster that allows the conversion of the ester-bond in glycerol-ester compound to the ether-bond, as present in *Acidobacteria*, across different bacterial phyla. They propose that this gene cluster originated in the δ-proteobacterial strains of the order *Myxococales*, where it would be responsible for the formation of IDA-MGE (Lorenzen et al., 2014). Although several bio-indicator OTUs are identified at the three sites within the order *Myxococcales* (Fig. 5), there is no clear phylogenetic distinction between high and low pH soils within the *Myxococcales* (Supp. Table 4, 5, 6). Further studies that evaluate the presence of brGDGTs in *Myxococcales*, and their link with their phylogeny, are needed to confirm their role as brGDGT producers. Until then, our findings support *Acidobacteria* as a likely candidate for the production of brGDGT lipids in soils.

4.3. Effect of soil chemistry on brGDGT-based proxies

Based on our local studies, we correlated the change in brGDGT concentration and fractional abundance with changes in soil pH and/or calcium (Table 1), and tentatively linked this to a change in (Acido)bacterial community composition. We will now evaluate whether the change in the fractional abundance of the brGDGT lipids has an effect on the brGDGT-based pH and temperature proxies CBT′ and MBT'_{5ME}. At all three sites, the pH proxies CBT′ and DC′ reflect the increase of 6-methyl brGDGTs and CP 5-methyl brGDGTs with increasing pH (Figs. 1D–E, 3D–E, 4E–F), confirming the observation on the global scale (De Jonge et al., 2014a; Yang et al., 2015; Weijers et al., 2007a). Nevertheless, there are some differences between the sites. Although the range in pH values is similar between Ossekampen and Craibstone, the range in CBT′ values at Ossekampen (−1.3 to 0.3: Fig. 1D) is larger than that at Craibstone (−1.2 to −0.3: Fig. 3D) resulting from a relatively stronger response of 6-methyl brGDGTs to increasing soil pH in Ossekampen than at Craibstone.

While the relation between soil pH and the fractional abundance of 6-methyl and CP-containing brGDGTs is known, soil pH is not expected to have a direct effect on the degree of methylation of the 5-methyl brGDGTs, reflected by the MBT'_{5ME} proxy [De Jonge et al., 2014; Naafs et al., 2017a, Dearing Crampton-Flood et al., 2020]. However, at Ossekampen, we observe a strong step-wise shift in the MBT'_{5ME} values (0.46–0.62) between low pH (pH < 4.5) and high pH (pH > 6.5 [limed]) soils (Fig. 1F). At Craibstone MBT'_{5ME} values similarly range from 0.48 to 0.59, increasing linearly with soil pH (Fig. 3F). In contrast, high pH soils at ForHot have decreased MBT'_{5ME} values compared to low pH soils within the same temperature range (Fig. 4G). As this effect of soil pH on the MBT'_{5ME} is unexpected, we evaluate which compounds influence the MBT'_{5ME} values. At the three sites, variation in the MBT'_{5ME} values is mainly determined by brGDGTs Ia, IIa, and IIIa, as most MBT'_{5ME} values and the values of the ratio Ia/(Ia + IIa + IIIa) fall on the 1:1 line (Fig. 6A). In theory, an increase in alkalinity-promoted compounds does not affect the (simplified) MBT'_{5ME} ratio as long as the fractional abundance of brGDGTs Ia, IIa and IIIa decrease to the same extent (see Supp. Fig. 7A–C for a conceptual model). Any deviations in the coeval decrease of brGDGTs Ia, IIa, and IIIa will be reflected as offsets from the theoretical relations between Ia vs IIa, and Ia vs IIIa, and captured by different Ia/(Ia + IIa) and Ia/(Ia + IIIa) values for high and low pH soils (Supp. Fig. 7D, E; Supp. Table 7). Projecting this
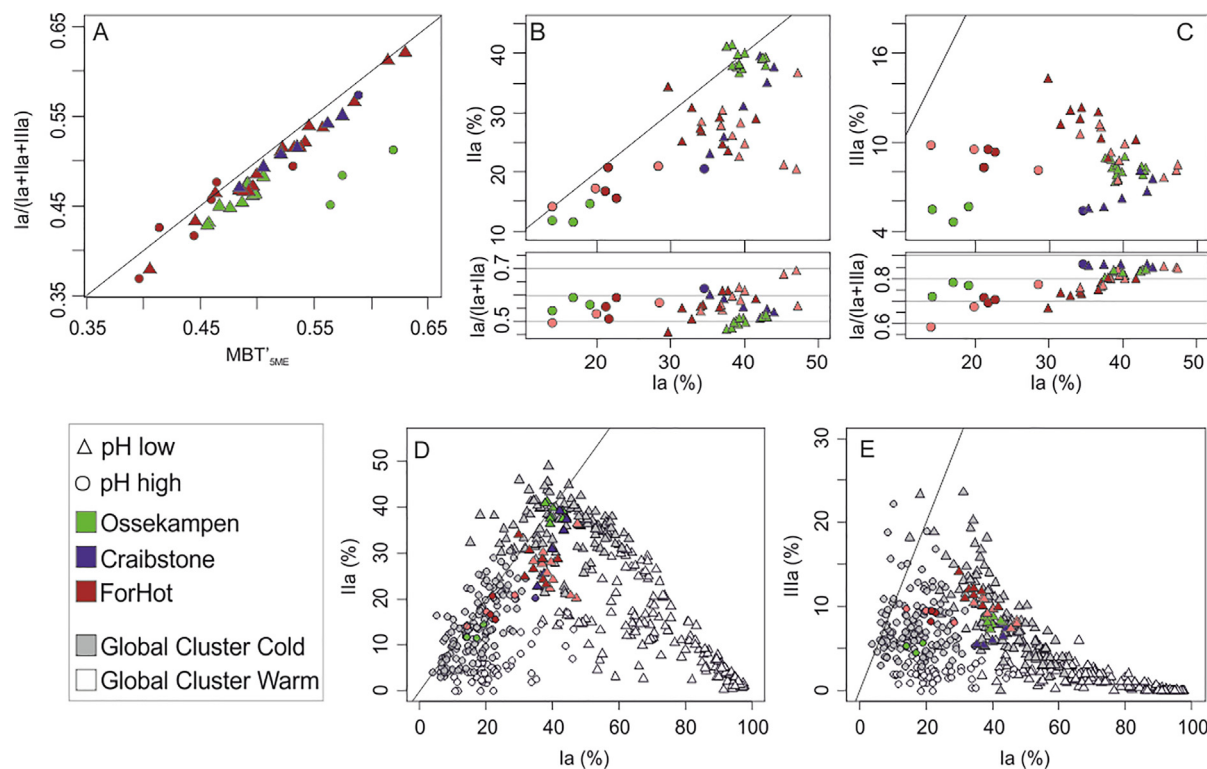
Fig. 6. (A) The MBT'_{5ME} [Eq. (1)] values plotted against the values of the ratio Ia/(Ia + IIa + IIIa), 1/1 line plotted. (B–E) The fractional abundance (%) of brGDGT Ia plotted against IIa (B and D) and IIIa (C and E), with 1/1 line plotted. B-C plots the fractional abundance of major brGDGT lipids at the study sites: Ossekampen [green], Craibstone [blue] and ForHot [brown – pink], differentiating between CBT′ < −0.37 [triangles] and CBT′ > −0.37 [circles]. Symbol color of ForHot soils reflects Mean Soil Temperature (MST), with brown < 7.6 °C (median MST) and pink > 7.6 °C. Subplots show the ratio values of Ia/(Ia + IIa) and Ia/(Ia + IIIa). D-E plots the fractional abundance of major brGDGT lipids in globally distributed Cluster Cold and Cluster Warm soils (grey and white symbols, respectively, after De Jonge et al., 2019), contrasting the soils with CBT′ < −0.37 [triangles] and CBT′ > −0.37 [circles]. Correlations between major brGDGT lipids are reported in Supp. Table 8. (For interpretation of the references to colour in this figure legend, the reader is referred to the web version of this article.)

insight on the local study sites, we see that at Craibstone, soils with an increasing soil pH show a stronger decrease of the fractional abundance of brGDGT IIa compared to Ia (Fig. 6B). This is seen as an increase in Ia/(Ia + IIa) ratio values moving from low pH to high pH soils (from 0.52 to 0.62), and drives the increase in MBT'_{5ME} values with pH (Fig. 3F). In the Ossekampen soils a large decrease in the relative abundance of both Ia and IIa is observed between low pH and high pH soils (Fig. 6B), that results in increased Ia/(Ia + IIa) ratio values in high pH (limed) soils, compared to low pH soils (0.45–0.60). However, while the fractional abundance of brGDGT Ia shows a relatively strong decrease in high pH Ossekampen soils, the fractional abundance of brGDGT IIIa barely changes. The Ia/(Ia + IIIa) ratio value consequently decreases between low and high pH Ossekampen soils (from 0.85 to 0.70; Fig. 6C). The opposite behavior of ratios Ia/(Ia + IIa) and Ia/(Ia + IIIa) results in Ia/(Ia + IIa + IIIa) values that are only slightly higher in high pH Ossekampen soils than in the low pH Ossekampen soils (Fig. 6A). The offset between Ia/(Ia + IIa + IIIa) values and the MBT'_{5ME} (Fig. 6A) indicates that the increase in the MBT'_{5ME} at higher pH Ossekampen soils is not only caused by the compounds Ia, IIa, or IIIa. In fact, the impact on the MBT'_{5ME} is amplified by the relative increase of CP-containing 5-methyl compounds Ib and IIb in high pH soils (Supp. Fig. 2).

At ForHot, both soil pH and MST have been shown to act on the brGDGT distributions. Notably, neither soil pH nor temperature correlate with MBT'_{5ME} values at this site (n = 25, p > 0.05, De Jonge et al., 2019). The absence of a temperature dependency at ForHot Cold Cluster soils, whereas this is present on a global scale within Cluster Cold soils ($r^2 = 0.28$, p < 0.01, n = 251; De Jonge et al., 2019), still remains to be explained. Possibly, the expected temperature effect on MBT'_{5ME} values at ForHot could be obscured by the impact of pH on brGDGT distributions. At ForHot, the fractional abundances of brGDGTs Ia and IIa change to the same relative extent between high and low pH soils (Fig. 6B and C), reflected by the similar values for Ia/(Ia + IIa) ratio between high pH and low pH soils (0.54–0.57, on average). On the other hand, the fractional abundance of brGDGT IIIa changes at a different rate, reflected by the dinstinct Ia/(Ia + IIIa) ratio values for low pH and high pH soils (respectively 0.79–0.70, on average). The difference between low pH soils and high pH soils at ForHot is also visible in the generally lower MBT'_{5ME} values for low pH soils compared to high pH soils at the same temperature range (Fig. 4G). Different from the Ossekampen and Craibstone sites, is the additional variation in the fractional abundances of brGDGTs IIa and IIIa. Fig. 6B and C show that those ForHot soils with MST > 7.6 °C (pink symbols) plot furthest away from the 1:1 line, which has been plotted as a reference. In other words, these soils have a lower fractional abundance of brGDGT IIa and IIIa, compared to the case where Ia, IIa and IIIa fractional abundances would be determined exclusively by the mechanism of dilution. This suggests that the decrease in fractional abundance of the brGDGTs IIa and IIIa in soils with MST > 7.6 °C is caused by the natural

temperature change at ForHot. To be able to see the impact of temperature on the MBT'_{5ME} values, the impact of pH needs to be removed. We do this by focusing on the soils with low pH values (pH < 6.1), where a more homogenous bacterial community is encountered (Fig. 2C). In this part of the dataset, the correlation between MBT'_{5ME} and soil temperature is almost significant (Fig. 4G, r = 0.43, p = 0.07, n = 19). This supports our interpretation that pH-dependent changes in MBT'_{5ME} values, can obscure a temperature dependency on a local scale. The detailed study of the dependency between simplified ratios Ia/(Ia + IIa), Ia/(Ia + IIIa) and pH changes, reflect the independent responses of brGDGT IIa and IIIa, that propagates in the MBT'_{5ME} values. At Craibstone and Ossekampen, MBT'_{5ME} increases with soil pH, while high pH soils at ForHot show a decreased MBT'_{5ME} value compared to low pH soils with the same temperature. The lack of a uni-directional response of brGDGTs Ia, IIa, and IIIa to changes in soil pH means that the influence of soil pH on MBT'_{5ME} values cannot be easily quantified or predicted.

4.4. Proposed impact of soil pH changes on global soils and paleoclimate archives

As the bacterial clades that change with soil pH in the experimental sites are also known to respond to pH on a global scale (Fierer and Jackson, 2006; Lauber et al., 2009; Rousk et al., 2010; Bartram et al., 2014), we postulate that brGDGT dependencies on a global scale will also vary with pH-dependent community changes. Extrapolating this insight to the global scale would allow to apprehend whether the observations made on a local scale, partially in artificially modified sites, fit the global pattern. Secondly, it can help understand the previously observed two-directional response of the MBT'_{5ME} to pH changes. However, in absence of studies that combine brGDGTs and bacterial community composition along global pH gradients, this extrapolation is not straightforward. Therefore, we assume that the pH-dependent brGDGT changes at ForHot, where a natural pH gradient is present, are also relevant on a global scale. At this site, the increase in concentration and fractional abundance of alkalinity-promoted compounds is marked by an average CBT' value of −0.37 (range between −0.42 and −0.32). Using this CBT' value as a threshold on a dataset of globally distributed soils and peats (Naafs et al., 2017a, 2017b, n = 446) to group high and a low pH soils, reveals that the variation observed in the local sites, spans most of the variation present within the Cluster Cold soils (CI < 0.64, following De Jonge et al., 2019) on a global scale (Fig. 6D–E). While the range in Ia/(Ia + IIa) and Ia/(Ia + IIIa) ratios between high pH and low pH soils within this cold cluster are similar, the dependencies between brGDGTs Ia, IIa and IIIa and soil pH are strikingly different (Supp. Table 8). For example, while the fractional abundance of brGDGTs Ia vs IIa shows a strong correlation for high pH soils (r = 0.72, p < 0.01), this correlation disappears in soils with a low pH (r = −0.04, p = 0.70) (Fig. 6D). In contrast, brGDGTs Ia and IIIa show a strong negative correlation in the Low pH soil cluster (r = −0.75,

p < 0.01), and no correlation for the High pH soil cluster (r = 0.01, p = 0.89) (Fig. 6E). Also within Cluster Warm soils (i.e. CI > 0.64; Fig. 6D, E) the dependency between brGDGTs Ia and IIa (r = 0.74, p < 0.01, r = −0.66, p < 0.01) and Ia and IIIa (r = 0.03, p > 0.8, r = −0.73, p < 0.01) is different for high and low pH soils, respectively (Supp. Table 8). As most Cluster Warm soils have CBT′ values below −0.37 (i.e. are low pH soils), the impact of soil pH changes possibly introduces less variation in the lipid signature of soils from this cluster. Regardless of the previous separation in Cluster Warm and Cluster Cold, a change in dependency between brGDGTs Ia, IIa and IIIa is observed between high pH and low pH soils (Supp. Table 8). We thus hypothesize that this change in dependency between the major brGDGT lipids on a global scale can be explained by the same bacterial community effect described on the local scale. Indeed, if brGDGT lipids in high pH and low pH soils are produced by a changed bacterial community, we don't expect them to be produced in the same relative abundance. The change in dependency between brGDGTs Ia, IIa and IIIa observed on the global scale, explains the change in ratio values between low pH and high pH soils on a local scale.

Published paleoclimate records where pH changes have been invoked to explain MBT′$_{5ME}$ changes in paleoclimate archives support the proposed global importance of the pH effect. The impact of pH on paleoclimate reconstructions will mostly depend on the likelihood of a soil to change pH (and associated brGDGT-producing bacterial community). As the nature of the soil pH buffer is linked to global climate patterns through precipitation and potential evaporation (Slessarev et al., 2016), the soil pH buffer has the potential to change as the climate changes. It is also known that erosion and depletion of minerals that buffer the soil or vegetation shifts can cause the soil chemistry to change with time. For example, a drop of 1–3 pH units with increasing soil age has been determined using soil chronosequences (e.g. Richardson et al., 2004 [pH drop from 6.8 to 3.9: 280 yr]; He et al., 2008 [6.5–4.5: 1800 ky]; Calero et al., 2009 [7.9–6.8: Holocene-Preholocene]; Bernasconi et al., 2011 [6.1–4.0: 150 yr]), and are often accompanied by large shifts in the bacterial community (e.g. Tarlera et al., 2008 [pH drops from 5.9 to 4.1: 77 ky], Williams et al., 2013 [pH drops from 7.6 to 3.6: 450 yr]; Ding et al., 2017 [pH drops from 7.4 to 5.9: 2 ky]). Furthermore, as plants can affect soil pH, changes in vegetation through time can cause large shift in soil pH. The change from Carex to Sphagnum vegetation in a Swiss peat sequence results in brGDGT signals corresponding with a decrease in reconstructed pH from 8.1 to 4 (Weijers et al., 2011). Similarly, Davies et al. (2021) report the MBT′$_{5ME}$ values might also be influenced by changes in a Canadian peat pH (MBT′$_{5ME}$ increases as pH decreases). Accordingly, Inglis et al. (2019) attribute an unexpected drop in MBT′$_{5ME}$-based temperatures at the onset of the PETM to an increase of ~2 pH units (5–7.5) in the production environment (UK, Cobham Lignite). Furthermore, the strong pH shift observed between lacustrine and peat horizons in a Holocene peat (NE China, Zheng et al., 2018; pH ranges from 7.8 to 4.3 [13 ky]), warrants caution when evaluating

brGDGT-based temperature records derived from sequences with changing lithology. Nevertheless, at most locations the pH of a given soil is generally well-buffered, even over the timescale of a climate change study. In paleosoils, published brGDGT-based reconstructed pH values generally do not indicate shifts from a High pH soil environment to a Low pH soil environment or vice versa (Zech et al., 2012 (loess, pH between 7.0 and 8.7 [125 ka], 6.8 and 8.1 [240 ka], 4.3 and 6.6 [80 ka], Peterse et al., 2014 (loess, 6.6–8.1 [130 ka]), Wang et al., 2017 (wetland, pH between 4.7 and 5.4 [30 ka]), Hutchings et al., 2019 (permafrost, pH between 4.5 and 6 [40 ka]).

Expanding the possible pH effect to the different production environments of brGDGTs, it is not clear yet whether pH will have the same effect on brGDGTs produced in mineral soils, peats and lacustrine systems. Peats are included in the global soil dataset (Fig. 6D, E) and show the same pH dependency as mineral soils (Dearing Crampton-Flood et al., 2020). We thus expect pH to have a similar effect on brGDGTs in peat, especially as they have been shown to respond to pH changes downcore (i.e. Weijers et al., 2011; Davies et al. (2021). However, pH has a lower correlation with CBT′ in peats (Naafs et al., 2017b), indicating that an (additional) environmental driver determines CBT′ values in peats. However, the relation between pH and brGDGTs, and CBT′ in particular, does not seem to hold in lacustrine systems (Loomis et al., 2014; Russell et al., 2018; Martínez-Sosa and Tierney, 2019; Raberg et al., 2021). This may be attributed to a change in the phylogenetic nature of the main bacteria in lake systems compared to in soils (i.e. Weber et al., 2018).

Although not all paleoclimate studies report proxy-based pH reconstructions, variability in pH values of up to 2 units is no exception. Therefore, the impact of soil pH on brGDGT patterns and MBT′$_{5ME}$ values needs to be considered when performing brGDGT-based climate reconstructions. We propose to evaluate this by evaluating changes in the calculated CBT′ values, and by comparing the cross plotted fractional abundances of brGDGT Ia and IIa, and Ia and IIIa (Fig. 6B, C). A change in the brGDGT dependency over time should be considered indicative of a soil-chemistry related change in the bacterial community, and changes in the MBT′$_{5ME}$ between high pH and low pH environments should thus be interpreted with care. Only when the impact of soil pH on the brGDGT distributions is determined to be minor, the MBT′$_{5ME}$ can be interpreted as a temperature proxy.

5. CONCLUSIONS

On the local scale 3 environmental drivers are identified to influence brGDGT distributions in Cluster Cold soils (De Jonge et al., 2019). Soil pH (or Ca^{2+} availability) appears the main driver of brGDGT variation, explaining a decrease in the concentration of brGDGTs Ia and IIa and an increase in 6-methyl brGDGTs (IIa′, IIb′, IIc′, IIIa′, IIIb′, IIIc′) and several CP containing 5-methyl brGDGTs (Ib, IIb, IIIb, IIIc) with increasing pH. Secondly, a poorly constrained environmental driver impacts the fractional abundance of brGDGT Ic. Finally, soil temperature

directly impacts the variation in the fractional abundance of brGDGT IIIa. Although no uniform pH threshold is encountered across the three experimental sites, each site does display a certain soil pH threshold (5.0–6.6) above which alkalinity-promoted compounds (brGDGTs Ib, IIb, IIc, IIIb, IIIc, IIa′, IIb′, IIc′, IIIa′, IIIb′, IIIc′) increase. The resulting change in the brGDGT distribution coincides with the main change in microbial community composition at each site. Taking the distribution of probable brGDGT precursor compounds into account, *Acidobacteria* subgroups 4 and 6 are identified as possible producers of CP 5-methyl brGDGTs and 6-methyl brGDGTs, respectively. *Acidobacteria* subgroups 1 and 3 are identified as probable producer of brGDGT Ia in low pH soils. However, as the complete suite of brGDGTs has not been recovered from culture studies (Sinninghe Damsté et al., 2018), this is only indirect evidence that Acidobacteria are relevant brGDGT producers in soils. The soil pH threshold is reflected by an independent change in the ratio values between Ia vs IIa and IIIa, which has an impact on MBT'_{5ME} values. The different ratio values between main brGDGTs Ia, IIa and IIIa on in pH low and pH high clusters can be explained by the proposed change in composition of the bacterial producers. In this case, we don't expect them to be produced in the same relative abundance. Although the local, experimental studies show that soil pH can strongly impact paleotemperature reconstructions, large natural pH shifts in soils require substantial changes in vegetation, climate or erosion patterns. As these changes are known to happen on timescales relevant for climate change reconstructions, we recommend using the brGDGTs-based CBT′ ratio and the diagnostic scatterplots between Ia, IIa and IIIa to evaluate (past) brGDGT distribution changes associated with soil pH. This will allow reliable paleotemperature reconstructions using the MBT'_{5ME} paleothermometer.

Declaration of Competing Interest

The authors declare that they have no known competing financial interests or personal relationships that could have appeared to influence the work reported in this paper.

APPENDIX A. SUPPLEMENTARY MATERIAL

Supplementary data to this article can be found online at https://doi.org/10.1016/j.gca.2021.06.037.

REFERENCES

Bartram A. K., Jiang X., Lynch M. D. J., Masella A. P., Nicol G. W., Dushoff J. and Neufeld J. D. (2014) Exploring links between pH and bacterial community composition in soils from the Craibstone Experimental Farm. *FEMS Microbiol. Ecol.* **87**, 403–415.

Bernasconi S. M., Bauder A., Bourdon B., Brunner I., Bünemann E., Chris I., Derungs N., Edwards P., Farinotti D., Frey B., Frossard E., Furrer G., Gierga M., Göransson H., Gülland K., Hagedorn F., Hajdas I., Hindshaw R., Ivy-Ochs S., Jansa J., Jonas T., Kiczka M., Kretzschmar R., Lemarchand E., Luster J., Magnusson J., Mitchell E. A. D., Venterink H. O., Plötze M., Reynolds B., Smittenberg R. H., Stähli M., Tamburini F., Tipper E. T., Wacker L., Welc M., Wiederhold J. G., Zeyer J., Zimmermann S. and Zumsteg A. (2011) Chemical and biological gradients along the damma glacier soil chronosequence, Switzerland. *Vadose Zone J.* **10**, 867.

Cáceres M. D. and Legendre P. (2009) Associations between species and groups of sites: indices and statistical inference. *Ecology* **90**, 3566–3574.

Calero J., Delgado R., Delgado G. and Martín-García J. M. (2009) SEM image analysis in the study of a soil chronosequence on fluvial terraces of the middle Guadalquivir (southern Spain). *Eur. J. Soil Sci.* **60**, 465–480.

Cassman N. A., Leite M. F. A., Pan Y., de Hollander M., van Veen J. A. and Kuramae E. E. (2016) Plant and soil fungal but not soil bacterial communities are linked in long-term fertilized grassland. *Sci. Rep.* **6**, 23680.

Costa O. Y. A., Oguejiofor C., Zühlke D., Barreto C. C., Wünsche C., Riedel K. and Kuramae E. E. (2020) Impact of different trace elements on the growth and proteome of two strains of Granulicella, class "Acidobacteriia". *Front. Microbiol.* **11**, 1227.

Dang X., Huan Y. B., Naafs D. A., Pancost R. D. and Xie S. (2016) Evidence of moisture control on the methylation of branched glycerol dialkyl glycerol tetraethers in semi-arid and arid soils. *Geochim. Cosmochim. Acta* **189**, 24–36.

Davies M. A., Blewett J., Naafs B. D. A. and Finkelstein S. A. (2021) Ecohydrological controls on apparent rates of peat carbon accumulation in a boreal bog record from the Hudson Bay Lowlands, northern Ontario, Canada. *Quaternary Res.*, 1–14.

Dearing Crampton-Flood E., Peterse F., Munsterman D. and Sinninghe Damsté J. S. (2018) Using tetraether lipids archived in North Sea Basin sediments to extract North Western European Pliocene continental air temperatures. *Earth Planet. Sci. Lett.* **490**, 193–205.

Dearing Crampton-Flood Emil, Tierney Jessica E., Peterse Francie, Kirkels Frédérique M. S. A. and Sinninghe Damsté J. S. (2020) BayMBT: A Bayesian calibration model for branched glycerol dialkyl glycerol tetraethers in soils and peats. *Geochim. Cosmochim. Acta* **268**, 142–159.

De Jonge C., Hopmans E. C., Stadnitskaia A., Rijpstra W. I. C., Hofland R., Tegelaar E. and Sinninghe Damsté J. S. (2013) Identification of novel penta- and hexamethylated branched glycerol dialkyl glycerol tetraethers in peat using HPLC–MS2, GC–MS and GC–SMB-MS. *Org. Geochem.* **54**, 78–82.

De Jonge C., Hopmans E. C., Zell C. I., Kim J.-H., Schouten S. and Sinninghe Damsté J. S. (2014a) Occurrence and abundance of 6-methyl branched glycerol dialkyl glycerol tetraethers in soils: Implications for palaeoclimate reconstruction. *Geochim. Cosmochim. Acta* **141**, 97–112.

De Jonge C., Stadnitskaia A., Hopmans E. C., Cherkashov G., Fedotov A. and Sinninghe Damsté J. S. (2014b) In situ produced branched glycerol dialkyl glycerol tetraethers in suspended particulate matter from the Yenisei River, Eastern Siberia. *Geochim. Cosmochim. Acta* **125**, 476–491.

De Jonge C., Radujković D., Sigurdsson B. D., Weedon J. T., Janssens I. and Peterse F. (2019) Lipid biomarker temperature proxy responds to abrupt shift in the bacterial community composition in geothermally heated soils. *Org. Geochem.* **137**, S0146638019301275.

DeCelles P. G., Castaneda I. S., Carrapa B., Liu J., Quade J., Leary R. and Zhang L. (2018) Oligocene-miocene great lakes in the India-Asia collision zone. *Basin Res.* **30**, 228–247.

Delgado-Baquerizo M., Oliverio A. M., Brewer T. E., Benavent-González A., Eldridge D. J., Bardgett R. D., Maestre F. T., Singh B. K. and Fierer N. (2018) A global atlas of the dominant bacteria found in soil. *Science* **359**, 320–325.

Ding L.-J., Su J.-Q., Li H., Zhu Y.-G. and Cao Z.-H. (2017) Bacterial succession along a long-term chronosequence of paddy soil in the Yangtze River Delta, China. *Soil Biol. Biochem.* **104**, 59–67.

Docherty K. M., Borton H. M., Espinosa N., Gebhardt M., Gil-Loaiza J., Gutknecht J. L. M., Maes P. W., Mott B. M., Parnell J. J., Purdy G., Rodrigues P. A. P., Stanish L. F., Walser O. N. and Gallery R. E. (2015) Key edaphic properties largely explain temporal and geographic variation in soil microbial communities across four biomes. *PLoS ONE* **10** e0135352.

Elberse W. Th., van den Bergh J. P. and Dirven J. G. P. (1983) Effects of use and mineral supply on the botanical composition and yield of old grassland on heavy-clay soil. *Neth. J. Agric. Sci.* **31**, 63–88.

Fierer N. and Jackson R. B. (2006) The diversity and biogeography of soil bacterial communities. *Proc. Natl. Acad. Sci.* **103**, 626–631.

Fierer N., Leff J. W., Adams B. J., Nielsen U. N., Bates S. T., Lauber C. L., Owens S., Gilbert J. A., Wall D. H. and Caporaso J. G. (2012) Cross-biome metagenomic analyses of soil microbial communities and their functional attributes. *Proc. Natl. Acad. Sci.* **109**, 21390–21395.

Harning David J., Curtin Lorele and Geirsdóttir Áslau, et al. (2020) Lipid biomarkers quantify Holocene summer temperature and ice cap sensitivity in Icelandic Lakes. *Geophys. Res. Lett.* **47**(3), 1–11.

He Y., Li D. C., Velde B., Yang Y. F., Huang C. M., Gong Z. T. and Zhang G. L. (2008) Clay minerals in a soil chronosequence derived from basalt on Hainan Island, China and its implication for pedogenesis. *Geoderma* **148**, 206–212.

He X., Su Y., Liang Y., Chen X., Zhu H. and Wang K. (2012) Land reclamation and short-term cultivation change soil microbial communities and bacterial metabolic profiles. *J. Sci. Food Agric.* **92**, 1103–1111.

Huguet C., Hopmans E. C., Febo-Ayala W., Thompson D. H., Sinninghe Damsté J. S. and Schouten S. (2006) An improved method to determine the absolute abundance of glycerol dibiphytanyl glycerol tetraether lipids. *Org. Geochem.* **37**, 1036–1041.

Hutchings J. A., Bianchi T. S., Kaufman D. S., Kholodov A. L., Vaughn D. R. and Schuur E. A. G. (2019) Millennial-scale carbon accumulation and molecular transformation in a permafrost core from Interior Alaska. *Geochim. Cosmochim. Acta* **253**, 231–248.

Hopmans E. C., Schouten S. and Sinninghe Damsté J. S. (2016) The effect of improved chromatography on GDGT-based palaeoproxies. *Org. Geochem.* **93**, 1–6.

Inglis G. N., Collinson M. E., Riegel W., Wilde V., Farnsworth A., Lunt D. J., Valdes P., Robson B. E., Scott A. C., Lenz O. K., Naafs B. D. A. and Pancost R. D. (2017) Mid-latitude continental temperatures through the early Eocene in western Europe. *Earth Planet. Sci. Lett.* **460**, 86–96.

Inglis G. N., Farnsworth A., Collinson M. E., Carmichael M. J., Naafs B. D. A., Lunt D. J., Valdes P. J. and Pancost R. D.

(2019) Terrestrial environmental change across the onset of the PETM and the associated impact on biomarker proxies: A cautionary tale. *Global Planet. Change* **181** 102991.

Jones R. T., Robeson M. S., Lauber C. L., Hamady M., Knight R. and Fierer N. (2009) A comprehensive survey of soil acidobacterial diversity using pyrosequencing and clone library analyses. *ISME J.* **3**, 442–453.

Kemp J. S., Paterson E., Gammack S. M., Cresser M. S. and Killham K. (1992) Leaching of genetically modified Pseudomonas fluorescens through organic soils: Influence of temperature, soil pH, and roots. *Biol. Fertil. Soils* **13**, 218–224.

Kielak A. M., Barreto C. C., Kowalchuk G. A., van Veen J. A. and Kuramae E. E. (2016) The ecology of acidobacteria: Moving beyond genes and genomes. *Front. Microbiol.* **7**, 744.

Killham K. (1990) Nitrification in coniferous forest soils. *Plant Soil* **128**, 31–44.

Kuramae E. E. and Costa O. Y. A. (2019) Acidobacteria. In *Encyclopedia of Microbiology* (ed. T. M. Schmidt), fourth ed. Academic Press, pp. 1–8.

Lauber C. L., Hamady M., Knight R. and Fierer N. (2009) Pyrosequencing-based assessment of soil pH as a predictor of soil bacterial community structure at the continental scale. *Appl. Environ. Microbiol.* **75**, 5111–5120.

Leblans, Niki I. W. (2016) Natural Gradients in Temperature and Nitrogen: Iceland Represents a Unique Environment to Clarify Longterm Global Change Effects on Carbon Dynamics. Joint PhD Thesis between Agricultural University of Iceland and University of Antwerp. Agric. Univ. Iceland.

Loomis S. E., Russell J. M., Eggermont H., Verschuren D. and Sinninghe Damsté J. S. (2014) Effects of temperature, pH and nutrient concentration on branched GDGT distributions in East African lakes: Implications for paleoenvironmental reconstruction. *Org. Geochem.* **66**, 25–37.

Lorenzen W., Ahrendt T., Bozhüyük K. A. J. and Bode H. B. (2014) A multifunctional enzyme is involved in bacterial ether lipid biosynthesis. *Nat. Chem. Biol.* **10**, 425–427.

Lynn T. M., Liu Q., Hu Y., Yuan H., Wu X., Khai A. A., Wu J. and Ge T. (2017) Influence of land use on bacterial and archaeal diversity and community structures in three natural ecosystems and one agricultural soil. *Arch. Microbiol.* **199**, 711–721.

Martínez-Sosa P. and Tierney J. E. (2019) Lacustrine brGDGT response to microcosm and mesocosm incubations. *Org. Geochem.* **127**, 12–22.

McMurdie and Holmes (2013) phyloseq: An R package for reproducible interactive analysis and graphics of microbiome census data. *PLoS ONE* **8**(4) e61217.

Menges J., Huguet C., Alcañiz J. M., Fietz S., Sachse D. and Rosell-Melé A. (2014) Influence of water availability in the distributions of branched glycerol dialkyl glycerol tetraether in soils of the Iberian Peninsula. *Biogeosciences* **11**, 2571–2581.

Naafs B. D. A., Gallego-Sala A. V., Inglis G. N. and Pancost R. D. (2017a) Refining the global branched glycerol dialkyl glycerol tetraether (brGDGT) soil temperature calibration. *Org. Geochem.* **106**, 48–56.

Naafs B. D. A., Inglis G. N., Zheng Y., Amesbury M. J., Biester H., Bindler R., Blewett J., Burrows M. A., del Castillo Torres D., Chambers F. M., Cohen A. D., Evershed R. P., Feakins S. J., Gałka M., Gallego-Sala A., Gandois L., Gray D. M., Hatcher P. G., Coronado E., Honorio N., Hughes P. D. M., Huguet A., Könönen M., Laggoun-Défarge F., Lähteenoja O., Lamentowicz M., Marchant R., McClymont E., Pontevedra-Pombal X., Ponton C., Pourmand A., Rizzuti A. M., Rochefort L., Schellekens J., De Vleeschouwer F. and Pancost R. D. (2017b) Introducing global peat-specific temperature and pH calibrations based on brGDGT bacterial lipids. *Geochim. Cosmochim. Acta* **208**, 285–301.

Naafs B. D. A., Rohrssen M., Inglis G. N., Lahteenoja O., Feakins S. J., Collinson M. E., Kennedy E. M., Singh P. K., Singh M. P., Lunt D. J. and Pancost R. D. (2018) High temperatures in the terrestrial mid-latitudes during the early Palaeogene. *Nat. Geosci.* **11**, 766.

Navarrete A. A., Kuramae E. E., de Hollander M., Pijl A. S., Veen V. A. J. and Tsai S. M. (2013) Acidobacterial community responses to agricultural management of soybean in Amazon forest soils. *FEMS Microbiol. Ecol.* **83**, 607–621.

Nicol G. W., Leininger S., Schleper C. and Prosser J. I. (2008) The influence of soil pH on the diversity, abundance and transcriptional activity of ammonia oxidizing archaea and bacteria. *Environ. Microbiol.* **10**, 2966–2978.

Niemann H., Stadnitskaia A., Wirth S. B., Gilli A., Anselmetti F. S., Sinninghe Damsté J. S., Schouten S., Hopmans E. C. and Lehmann M. F. (2012) Bacterial GDGTs in Holocene sediments and catchment soils of a high Alpine lake: application of the MBT/CBT-paleothermometer. *Clim. Past* **8**, 889–906.

Oksanen J., Blanchet F. G., Friendly M., Kindt R., Legendre P., McGlinn D., Minchin P. R., O'Hara R. B., Simpson G. L., Solymos P., Stevens M. H. H., Szoecs E. and Wagner H. (2019). Vegan: Community Ecology Package. R package version 2.5-6.

Pajares S., Escalante A. E., Noguez A. M., García-Oliva F., Martínez-Piedragil C., Cram S. S., Eguiarte L. E. and Souza V. (2016) Spatial heterogeneity of physicochemical properties explains differences in microbial composition in arid soils from Cuatro Cienegas, Mexico. *PeerJ* **4** e2459.

Pan Y., Cassman N., de Hollander M., Mendes L. W., Korevaar H., Geerts R. H. E. M., van Veen J. A. and Kuramae E. E. (2014) Impact of long-term N, P, K, and NPK fertilization on the composition and potential functions of the bacterial community in grassland soil. *FEMS Microbiol. Ecol.* **90**, 195–205.

Peterse F., Nicol G. W., Schouten S. and Sinninghe Damsté J. S. (2010) Influence of soil pH on the abundance and distribution of core and intact polar lipid-derived branched GDGTs in soil. *Org. Geochem.* **41**, 1171–1175.

Peterse F., van der Meer J., Schouten S., Weijers J. W. H., Fierer N., Jackson R. B., Kim J.-H. and Sinninghe Damsté J. S. (2012) Revised calibration of the MBT–CBT paleotemperature proxy based on branched tetraether membrane lipids in surface soils. *Geochim. Cosmochim. Acta* **96**, 215–229.

Peterse F., Martínez-García A., Zhou B., Beets C. J., Prins M. A., Zheng H. and Eglinton T. I. (2014) Molecular records of continental air temperature and monsoon precipitation variability in East Asia spanning the past 130,000 years. *Quat. Sci. Rev.* **83**, 76–82.

Pitcher A., Hopmans E. C., Schouten S. and Sinninghe Damsté J. S. (2009) Separation of core and intact polar archaeal tetraether lipids using silica columns: Insights into living and fossil biomass contributions. *Org. Geochem.* **40**, 12–19.

Qian P. and Schoenau J. J. (2011) Practical applications of ion exchange resins in agricultural and environmental soil research. *Can. J. Soil Sci.* **82**, 9–21.

R Core Team (2018) *R: A language and environment for statistical computing*. R Foundation for Statistical Computing, Vienna, Austria.

Raberg J. H., Harning D. J., Crump S. E., de Wet G., Blumm A., Kopf S., Geirsdóttir Á., Miller G. H. and Sepúlveda J. (2021) Revised fractional abundances and warm-season temperatures substantially improve brGDGT calibrations in lake sediments. *Biogeosci.* **18**(12), 3579–3603.

Radujković D., Verbruggen E., Sigurdsson B. D., Leblans N. I. W., Janssens I. A., Vicca S. and Weedon J. T. (2018) Prolonged exposure does not increase soil microbial community compositional response to warming along geothermal gradients. *FEMS Microbiol. Ecol.* **94**.

Ramirez K. S., Leff J. W., Barberán A., Bates S. T., Betley J., Crowther T. W., Kelly E. F., Oldfield E. E., Shaw E. A., Steenbock C., Bradford M. A., Wall D. H. and Fierer N. (2014) Biogeographic patterns in below-ground diversity in New York City's Central Park are similar to those observed globally. *Proc. R. Soc. B* **281**, 20141988.

Richardson S. J., Peltzer D. A., Allen R. B., McGlone M. S. and Parfitt R. L. (2004) Rapid development of phosphorus limitation in temperate rainforest along the Franz Josef soil chronosequence. *Oecologia* **139**, 267–276.

Rousk J., Baath E., Brookes P. C., Lauber C. L., Lozupone C., Caporaso J. G., Knight R. and Fierer N. (2010) Soil bacterial and fungal communities across a pH gradient in an arable soil. *ISME J.* **4**, 1340–1351.

Russell J. M., Hopmans E. C., Loomis S. E., Liang J. and Sinninghe Damsté J. S. (2018) Distributions of 5- and 6-methyl branched glycerol dialkyl glycerol tetraethers (brGDGTs) in East African lake sediment: Effects of temperature, pH, and new lacustrine paleotemperature calibrations. *Organic Geochemistry* **117**, 56–69.

Sangiorgi F., Bijl P. K., Passchier S., Salzmann U., Schouten S., McKay R., Cody R. D., Pross J., van de Flierdt T., Bohaty S. M., Levy R., Williams T., Escutia C. and Brinkhuis H. (2018) Southern Ocean warming and Wilkes Land ice sheet retreat during the mid-Miocene. *Nat. Commun.* **9**, 317.

Sigurdsson B. D., Leblans N. I. W., Dauwe S., Gudmundsdottir E., Gundersen P., Gunnarsdottir G. E., Holmstrup M., Ilieva-Makulec K., Katterer T., Marteinsdottir B.-S., Maljanen M., Oddsdottir E. S., Ostonen I., Penuelas J., Poeplau C., Richter A., Sigurdsson P., Van Bodegom P., Wallander H., Weedon J. and Janssens I. (2016) Geothermal ecosystems as natural climate change experiments: The ForHot research site in Iceland as a case study. *Iceland. Agric. Sci.* **29**, 53–71.

Sinninghe Damsté J. S., Hopmans E. C., Pancost R. D., Schouten S. and Geenevasen J. A. J. (2000) Newly discovered non-isoprenoid glycerol dialkyl glycerol tetraether lipids in sediments. *Chem. Commun.* **17**, 1683–1684.

Sinninghe Damsté J. S., Ossebaar J., Abbas B., Schouten S. and Verschuren D. (2009) Fluxes and distribution of tetraether lipids in an equatorial African lake: Constraints on the application of the TEX86 palaeothermometer and BIT index in lacustrine settings. *Geochim. Cosmochim. Acta* **73**, 4232–4249.

Sinninghe Damsté J. S., Rijpstra W. I. C., Hopmans E. C., Weijers J. W. H., Foesel B. U., Overmann J. and Dedysh S. N. (2011) 13, 16-dimethyl octacosanedioic acid (iso-diabolic acid), a common membrane-spanning lipid of Acidobacteria subdivisions 1 and 3. *Appl. Environ. Microbiol.* **77**, 4147–4154.

Sinninghe Damsté J. S., Rijpstra W. I. C., Hopmans E. C., Foesel B. U., Wüst P. K., Overmann J., Tank M., Bryant D. A., Dunfield P. F., Houghton K. and Stott M. B. (2014) Ether- and ester-bound iso-diabolic acid and other lipids in members of acidobacteria subdivision 4. *Appl. Environ. Microbiol.* **80**, 5207–5218.

Sinninghe Damsté J. S., Rijpstra W. I. C., Foesel B. U., Huber K. J., Overmann J., Nakagawa S., Kim J. J., Dunfield P. F., Dedysh S. N. and Villanueva L. (2018) An overview of the occurrence of ether- and ester-linked iso-diabolic acid membrane lipids in microbial cultures of the Acidobacteria: Implications for brGDGT paleoproxies for temperature and pH. *Org. Geochem.* **124**, 63–76.

Slessarev E. W., Lin Y., Bingham N. L., Johnson J. E., Dai Y., Schimel J. P. and Chadwick O. A. (2016) Water balance creates a threshold in soil pH at the global scale. *Nature* **540**, 567–569.

Super J. R., Chin K., Pagani M., Li H., Tabor C., Harwood D. M. and Hull P. M. (2018) Late Cretaceous climate in the Canadian

Arctic: Multi-proxy constraints from Devon Island. *Paleogeogr. Paleoclimatol. Paleoecol.* **504**, 1–22.

Tarlera S., Jangid K., Ivester A. H., Whitman W. B. and Williams M. A. (2008) Microbial community succession and bacterial diversity in soils during 77 000 years of ecosystem development. *FEMS Microbiol. Ecol.* **64**, 129–140.

Walinga I., Van Der Lee J. J., Houba V. J. G., Van Vark W. and Novozamsky I. (1995) Digestion in tubes with H2SO4-salicylic acid- H2O2 and selenium and determination of Ca, K, Mg, N, Na, P, Zn. In *Plant Analysis Manual* (eds. I. Walinga, J. J. Van Der Lee, V. J. G. Houba, W. Van Vark and I. Novozamsky). Springer, Netherlands, Dordrecht, pp. 7–45.

Walker T. W. N., Janssens I. A., Weedon J. T., Sigurdsson B. D., Richter A., Peñuelas J., Leblans N. I. W., Bahn M., Bartrons M., Jonge C. D., Fuchslueger L., Gargallo-Garriga A., Gunnarsdóttir G. E., Marañón-Jiménez S., Oddsdóttir E. S., Ostonen I., Poeplau C., Prommer J., Radujković D., Sardans J., Sigurðsson P., Soong J. L., Vicca S., Wallander H., Ilieva-Makulec K. and Verbruggen E. (2020) A systemic overreaction to years versus decades of warming in a subarctic grassland ecosystem. *Nat. Ecol. Evol.* **4**, 101–108.

Wallis P. D., Haynes R. J., Hunter C. H. and Morris C. D. (2010) Effect of land use and management on soil bacterial biodiversity as measured by PCR-DGGE. *Appl. Soil Ecol.* **46**, 147–150.

Wang M., Zheng Z., Man M., Hu J. and Gao Q. (2017) Branched GDGT-based paleotemperature reconstruction of the last 30,000 years in humid monsoon region of Southeast China. *Chem. Geol.* **463**, 94–102.

Wang M., Zheng Z., Zong Y., Man M. and Tian L. (2019) Distributions of soil branched glycerol dialkyl glycerol tetraethers from different climate regions of China. *Sci. Rep.* **9**, 2761.

Ward J. H. (1963) Hierarchical grouping to optimize an objective function. *J. Am. Stat. Assoc.* **58**, 236–244.

Watson B. I., Williams J. W., Russell J. M., Jackson S. T., Shane L. and Lowell T. V. (2018) Temperature variations in the southern Great Lakes during the last deglaciation: Comparison between pollen and GDGT proxies. *Quat. Sci. Rev.* **182**, 78–92.

Weber Y., Damsté J. S. S., Zopfi J., Jonge C. D., Gilli A., Schubert C. J., Lepori F., Lehmann M. F. and Niemann H. (2018) Redox-dependent niche differentiation provides evidence for multiple bacterial sources of glycerol tetraether lipids in lakes. *PNAS* **115**, 10926–10931.

Weijers J. W. H., Schouten S., Hopmans E. C., Geenevasen J. A. J., David O. R. P., Coleman J. M., Pancost R. D. and Damste J. S. S. (2006) Membrane lipids of mesophilic anaerobic bacteria thriving in peats have typical archaeal traits. *Environ. Microbiol.* **8**, 648–657.

Weijers J. W. H., Schouten S., van den Donker J. C., Hopmans E. C. and Sinninghe Damsté J. S. (2007a) Environmental controls on bacterial tetraether membrane lipid distribution in soils. *Geochim. Cosmochim. Acta* **71**, 703–713.

Weijers J. W. H., Schefuss E., Schouten S. and Sinninghe Damsté J. S. (2007b) Coupled thermal and hydrological evolution of tropical Africa over the last deglaciation. *Science* **315**, 1701–1704.

Weijers J. W. H., Steinmann P., Hopmans E. C., Schouten S. and Sinninghe Damsté J. S. (2011) Bacterial tetraether membrane lipids in peat and coal: Testing the MBT–CBT temperature proxy for climate reconstruction. *Org. Geochem.* **42**, 477–486.

Williams M. A., Jangid K., Shanmugam S. G. and Whitman W. B. (2013) Bacterial communities in soil mimic patterns of vegetative succession and ecosystem climax but are resilient to change between seasons. *Soil Biol. Biochem.* **57**, 749–757.

Xia Z., Bai E., Wang Q., Gao D., Zhou J., Jiang P. and Wu J. (2016) Biogeographic distribution patterns of bacteria in typical Chinese forest soils. *Front. Microbiol.* **7**, 1106.

Yang H., Lü X., Ding W., Lei Y., Dang X. and Xie S. (2015) The 6-methyl branched tetraethers significantly affect the performance of the methylation index (MBT′) in soils from an altitudinal transect at Mount Shennongjia. *Org. Geochem.* **82**, 42–53.

Zech R., Gao L., Tarozo R. and Huang Y. (2012) Branched glycerol dialkyl glycerol tetraethers in Pleistocene loess-paleosol sequences: Three case studies. *Org. Geochem.* **53**, 38–44.

Zheng Y., Pancost R. D., Naafs B. D. A., Li Q., Liu Z. and Yang H. (2018) Transition from a warm and dry to a cold and wet climate in NE China across the Holocene. *Earth Planet. Sci. Lett.* **493**, 36–46.

Associate editor: Josef P. Werne